RSC Advances

ROYAL SOCIETY OF CHEMISTRY

www.rsc.org/advances

RCS Advances

RSCPublishing

REVIEW

Luminescent Lanthanide Coordination Polymers for Photonic Applications

Cite this: DOI: 10.1039/x0xx00000x

Y. Hasegawa* and T. Nakanishi

Received 00th January 2012,
Accepted 00th January 2012

DOI: 10.1039/x0xx00000x

www.rsc.org/

Luminescent lanthanide coordination polymers composed of lanthanide ions and organic joint ligands exhibit characteristic photophysical and thermostable properties that are different from typical organic dyes, luminescent metal complexes, and semiconductor nanoparticles. Various types of luminescent Eu(III) and Tb(III) coordination polymers have been reported to date. One-, two-, and three-dimensional alternating sequences of lanthanide ions and organic ligands exhibit remarkable characteristics as novel organic materials with various structures, and unique physical properties. In this review, the characteristic structures, photophysical properties, and photonic applications for organic display devices, triboluminescent materials, thermosensors, color and brightness tuning, new type organogels, future magneto-optical materials, luminescent organo-nanoparticles, and energy transfer process of lanthanide coordination polymers are introduced.

1. Introduction

The lanthanides are composed of lanthanum (La) and 14 other elements (Ce, Pr, Nd, Pm, Sm, Eu, Gd, Tb, Dy, Ho, Er, Tm, Yb, and Lu).[1] Lanthanides are typically represented by the symbol Ln. The lanthanides in the stable III oxidation state are simply characterized by the electronic structure in 4f orbital. The 4f orbital is shielded by the outer $5s^2$ and $5p^2$ orbitals. From this reason, shift of the wavelength of the electronic transitions depended on the host media are much slight. The energy levels of the trivalent lanthanide ion are given in Fig. 1. The energy levels presented in Fig. 1 are split by the crystal or ligand field. This splitting energy is very small due to shielding by the outer electrons in $5s^2$ and $5p^2$ orbitals. Although the ligand field strength of transition metal ions (d^n) is fundamentally several tens of thousands of cm^{-1}, the ligand field strength for Ln(III) ions (f^n) amounts to several hundreds of cm^{-1}. In a configurational coordinate diagram, energy levels in 4f orbital appear as parallel parabolas (small off-set case) because the 4f electrons are well shielded from outer filled $5s^2$ and $5p^2$ orbitals.[2] Thus, electronic transitions in absorption and emission processes show sharp spectral lines. The radiative emission of for Ln(III) ions comes mainly from the electric dipole transition. The electric transitions in the inner $4f^n$ orbital of free ions are forbidden because they do not correspond to a

Faculty of Engineering, Hokkaido University, Sapporo 060-8628, Japan. Eimail: hasegaway@eng.hokudai.ac.jp

Yasuchika Hasegawa obtained his Ph.D (1997) at the Garaduate School of Engineering, Osaka University and was researcher (1994 – 1999) at New Japan Chemical Co. Ltd. He was assistant professor (1999 – 2005) at Osaka University and associate professor (2005 – 2010) at Nara Institute of Science and Technology. Since 2010 he has been a professor at Hokkaido University. He received Young Award of Rare Earth Society of Japan (2006), The JPA (Japanese Photochemistry Association) Award for Young photochemists (2010), Academic Awards of NAIST (2009), the JPA Award (2013), and the CSJ (The Chemical Society of Japan) Award for Creative Work (2014). His major is study on lanthanide photochemistry.

Takayuki Nakanishi obtained his Ph.D (2009) at Graduate School of Human and Environmental Studies, Kyoto University. He held a Research Fellow of the Japan Society for the Promotion of Science (JSPS) (2010) at department of materials Science and Technology, Nagaoka University of Technology. Since 2011 he has been a assistant professor at faculty of engineering, Hokkaido University. His interests are luminescent glass ceramics, phosphors, non-crystals, metal complexes, and clusters containing lanthanide ions. He is now studying on luminescent and opto-magnetic materials of lanthanide clusters.

change of parity. However, the transitions are partially allowed by mixing of the 4f orbital (odd parity) and 5d orbital (even parity) under the ligand field. The parity does not change significantly in such a transition; therefore, the lifetime of the excited state is long (ca. 10 ms). Lanthanides with characteristic 4f orbitals exhibit attractive photophysical properties.[3]Inorganic phosphors and coordination compounds including lanthanide ions have also been synthesized and their resulting emission properties have been explored.

Recently, metal organic frameworks (MOFs) composed of lanthanide ions and organic ligands, Ln-MOFs, have been widely studied.[4-7] At the present stage, various types of luminescent Ln-MOFs have been reported. MOFs provide characteristic frameworks with three-dimensional cavities that act to encapsulate metals and/or molecules (Fig. 2a).[8-19] Such cavities are applied as nanoscale sensors for metal ions and gas or organic molecules based on the host-guest chemistry. Chandler et al. described CO_2 gas sensors that employ luminescent Ln-MOFs.[20] Liu et al. and Pan et al. have demonstrated Ag^+ sensors based on water-soluble Ln-MOFs.[21,22]
In addition, Roch and Carlos have provided a review on luminescent multifunctional lanthanides-based Ln-MOFs.[24] Roch and Carlos have also provides the review for luminescent Rocha and colleagues have studied the sensing properties of alternating steams of air saturated with ethanol using luminescent Ln-MOFs powders.[23] multifunctional lanthanides-based metal-organic frameworks, Ln-MOFs.[24]

On the other hand, coordination polymers composed of luminescent lanthanide ions and organic joint ligands have also attracted considerable attention in the fields of coordination chemistry, inorganic chemistry, supramolecular chemistry, polymer and material science. One-, two-, and three-dimensional alternating sequences of metal ions and organic ligands (Fig. 2b) exhibit remarkable characteristics as novel organic-inorganic hibrid materials with various structures, and unique physical properties that can be easily prepared by the combination of lanthanide ions and organic ligands. The characteristic network structures lead to a tight packing formation of both lanthanide ions and organic molecules, which results in thermostable structures for photonic applications. Herein, we focus on coordination polymers formed with lanthanide ions.

2. Linker ligands for formation of lanthanide coordination polymers

Lanthanide coordination polymers are generally constructed from lanthanide ions and small organic joint parts with two coordination sites. Figure 3 shows various types of linker polymer ligands. The most popular linker ligands include carboxylic groups in the polymer. The carboxylic group is a typical functional group that acts as a coordination site for the formation of metal complexes. The carboxylic acid group acts as an organo-linker site between lanthanide ions. The connection of lanthanide ions and carboxylic groups leads to the tight packing structure of the lanthanide coordination polymers. The network structure of a Tb(III) coordination polymer with benzene-carboxylate linkers was characterized using single crystal X-ray diffraction (XRD) analysis in 2001 (Fig. 3a).[25] Daiguebonne and Bünzli reported micro- and nanosized particles of lanthanide coordination polymers linked with benzene-*p*-dicarboxylates.[26] The Tb(III)-containing coordination polymers exhibit large emission quantum yields up to 43%. They also prepared polyvinylpyrrolidone nanoparticles doped with $[Ln_2(C_8H_4O_4)_3(H_2O)_4]_n$ ($C_8H_4O_4$: benzene-*p*-dicarboxylate) (Fig. 3b and Fig. 4a). Du and colleagues reported the helical shapes of luminescent lanthanide coordination polymers constructed with benzene-*m*-dicarboxylates (Fig. 3c).[27] Bettencourt-Dias presented two-dimensional coordination polymers composed of lanthanide ions and benzene-*m*-dicarboxylates (isophthalic acid) or thiophene-derivatized isophthalic acid (Fig. 4b),[28] where the emission quantum yields of the excited Tb(III) coordination polymers with a π–π* transition were estimated to be 3.6 and 7.5%, respectively. Naphthyl-, imidazol-, and pyridyl-type linkers with dicarboxylate groups have also been reported (Figs. 3d and 3e).[29-32] Lanthanide coordination polymers linked with tricarboxylate ligands (benzene and pyridine-2,4,6-tricarboxylate) were reported by Cheng and coworkers (Figs. 3d and 3e).[33]

We have reported luminescent lanthanide coordination polymers linked with bidentate phosphine oxide groups. The bidentate phosphine oxide groups are linked with organo-aromatic compounds (Figs. 3f, 3g, and 3h).[34,35] The vibrational frequency of phosphine oxide (P=O: 1125 cm^{-1}) is smaller than that of the carboxylic group (C=O: ca. 1600 cm^{-1}). The smaller vibrational frequency of the coordination site in lanthanide complexes and coordination polymers leads to the suppression of vibrational relaxation from the excited state, which results in a smaller radiative rate constant (k_{nr}) and a higher emission quantum yield.[36-44] We have previously reported the importance of phosphine oxide as a coordination site.[45-57] Bidentate phosphine oxide ligands are effective for the preparation of strongly luminescent lanthanide coordination polymers that exhibit large emission quantum yields up to 70% under 4f-4f excitation (refer to section 3).[34]

Nitrogen atoms in aromatic compounds are also used for the formation of lanthanide coordination polymers. Wang and coworkers have prepared Tb(III) coordination polymers with benzene-monocarboxylates and 4,4'-bipyridine (Fig. 3i).[25] The Tb(III) coordination polymer has a grid-type structure with three-dimensional networks (refer to section 4.1).

Luminescent lanthanide coordination polymers linked with nucleotides have also been reported for the imaging of biomaterials (Fig. 3j and Fig. 4).[58] The lanthanide coordination polymers form nanoparticles with diameters of 41 nm in water. The authors suggested that the coordination sites in the nucleotides could be composed of phosphoric acid and nitrogen atoms.

3. Thermo-stability

Typical luminescent organic molecules, such as rhodamine and coumarin, are decomposed at temperatures under 200 °C in air. The decomposition temperatures of typical luminescent lanthanide complexes are also under 250 °C. The thermal stability of luminescent materials is required for industrial preparation processes under high temperatures around 250 °C, such as material molding processes and solder dissolution processes for the construction of electronic devices. The use of luminescent lanthanide complexes in photonic applications requires thermostable structures.

There has recently been a focus on luminescent lanthanide coordination polymers as thermostable luminescent materials for industrial applications. Lanthanide coordination polymers have tight packing structures, which leads to effective thermostable properties in air. Marchetti and coworkers reported a thermo-stable coordination polymer composed of Eu(III) ions and organic 4-acylpyrazolone ligands.[59] Wang also reported that lanthanide coordination polymer attached with glutaric acid shows higher decomposition point (> 300 °C).[60] Reddy has also reported thermally stable lanthanide coordination polymers with 4-(dipyridine-2-

yl)aminobenzoate ligands (thermal decomposition point = 450 °C).[61] However, these lanthanide coordination compounds have low emission quantum yields of less than 20%. The relatively low emission quantum efficiencies of these coordination polymers are attributed to a nonradiative transition via vibrational relaxation of high-vibrational frequency O-H bonds in the organic linker ligands. Luminescent coordination polymers with both high thermostability and emission quantum efficiency are required as novel organophosphors for future optoelectronic devices.

3.1 CH/F and CH/π interactions

We have considered that the introduction of low vibrational frequency ligands as the organic linker part into the lanathanide polymer system leads to effective luminescence of lanthanide coordination polymer. Strongly luminescent lanthanide complexes composed of low vibrational frequency hexafluoroacetylacetonate (hfa) and bidentate phosphine oxide ligands have been reported. [34-57] We have also proposed that the introduction of aromatic aryl groups in the linker part of a lanthanide coordination polymer would be required for the construction of thermostable organophosphor compounds with intermolecular interactions such as CH/F, π–π, and CH/π interactions. Based on these photophysical and chemical considerations, we have reported novel organophosphor coordination polymers composed of Eu(III) and three types of aryl units; $[Eu(hfa)_3(dpb)]_n$, $[Eu(hfa)_3(dpbp)]_n$ (**Fig. 5**), and $[Eu(hfa)_3(dppcz)]_n$ (dpb: 1,4-bis(diphenylphosphoryl)benzene, dpbp: 4,4'-bis(diphenyl-phosphoryl)biphenyl, dppcz: 3,6-bis(diphenylphosphoryl)-9-phenyl-carbazole).[34]

The three-dimensional network structures between the coordination polymers were determined by single crystal XRD analysis. The ORTEP view shows that the phosphine oxide ligand acts as a bidentate bridge between lanthanide ions in one-dimensional polymeric chains (**Fig. 6**). The coordination sites of $[Eu(hfa)_3(dpb)]_n$, $[Eu(hfa)_3(dpbp)]_n$, and $[Eu(hfa)_3(dppcz)]_n$ comprise three hfa ligands and two phosphine oxide units. X-ray analysis also reveals intermolecular interactions between one-dimensional polymeric chains. In one unit, two CH/F interactions and one CH/π interaction were identified for $[Eu(hfa)_3(dppcz)]_n$. In addition, CH/π interactions in the polymer chains of $[Eu(hfa)_3(dpbp)]_n$ were also observed. These tight-binding structures are directly linked to their thermal stability. Thermogravimetric analysis (TGA) and differential scanning calorimetry (DSC) were conducted to estimate the thermal stability of the Eu(III) coordination polymers. The thermal decomposition points from the TGA thermograms were 261, 308, and 300 °C for $[Eu(hfa)_3(dpb)]_n$, $[Eu(hfa)_3(dpbp)]_n$, and $[Eu(hfa)_3(dppcz)]_n$, respectively. In contrast, the thermal decomposition point of the reported Eu(III) complex, $[Eu(hfa)_3(biphepo)]$ (biphepo: 1,1'-biphenyl-2,2'-diylbis(di-phenylphosphine oxide)),[46] was reported to be 230 °C. The high thermal stability of $[Eu(hfa)_3(dpbp)]_n$ and $[Eu(hfa)_3(dppcz)]_n$ is due to the tight-packing structure supported by a combination of CH/F and CH/π interactions. The binding energies of CH/F (hydrogen bond) and CH/π interactions are generally known to be 10–30 kJ mol^{-1} and 2–10 kJ mol^{-1}, respectively.[62] The enhanced photostability of organic molecules containing hydrogen bonds has been reported.[63] We consider that a combination of both CH/F and CH/π interactions in such coordination polymers is effective for the construction of thermostable organophosphor compounds.

$[Eu(hfa)_3(dpb)]_n$, $[Eu(hfa)_3(dpbp)]_n$, and $[Eu(hfa)_3(dppcz)]_n$ have high emission quantum yields (Φ_{Ln} $[Eu(hfa)_3(dpb)]_n$ = 70%, Φ_{Ln} $[Eu(hfa)_3(dpbp)]_n$ = 72%, Φ_{Ln} $[Eu(hfa)_3(dppcz)]_n$ = 83%). The nonradiative rate constants (k_{nr}) for the Eu(III) coordination polymers ($1.8–3.3\times10^2$ s^{-1}) were approximately ten times smaller than that for $[Eu(hfa)_3(H_2O)_2]$ (3.7×10^3 s^{-1}). The smaller k_{nr} for the Eu(III) coordination polymers is attributed to the suppression of vibrational relaxation. Therefore, we consider that introduction of the low-vibrational frequency phosphine oxide ligand and aromatic aryl group for intermolecular interactions in the coordination polymer system is effective for the preparation of organophosphor compounds with high thermal stabilities and high emission quantum yields.

These new phosphor compounds are expected to be employed in optics applications such as luminescent plastics, displays, and optoelectronic devices. Such lanthanide coordination polymers with CH/F and CH/π interaction networks could also open up new fields in supramolecular chemistry, polymer science, and molecular engineering.

3.2 Calcination

Du and co-workers have reported on luminescent lanthanide coordination polymer after heat-treatment. The lanthanide coordination polymer are composed of lanthanide(III) ions (Eu(III) or Tb(III) and m-H_2BDC (1,3-benzenedicarboxylic acids), $[Ln_4(m\text{-}BDC)_6(H_2O)_4(DMF)] \cdot (H_2O)_2(DMF)$.[27] X-ray single crystal analysis of this compound indicates that the lanthanide coordination polymer is isomorphous and each displays a layered structure with helical polymer chains (Fig. 8).

According to the thermal stability, TG and DSC analysis of the lanthanide coordination polymers has been performed. A weight loss of 14.18% occurs from room temperature to 320 °C (calcd 13.75%), which corresponds to the loss of coordinated and lattice solvent molecules. The decomposition point of coordination structure is at around 520 °C.

After calcination at 450 °C, there exists no endothermic peak for the structural collapse until 520 °C. Unfortunately, they have also reported that the emission quantum yield of $[Tb_4(m\text{-}BDC)_6]$ with calcination at 298 K (11 %) was smaller than that of $[Tb_4(m\text{-}BDC)_6(H_2O)_4(DMF)] \cdot (H2O)2(DMF)$ (23 %). We feel that keep of the coordination frame is a key factor for strong luminescence properties of lanthanide coordination polymer. Reference from S. Du. [27]

4. Photonic Applications

Luminescent lanthanide coordination polymers have characteristic network structures composed of lanthanide ions and functional organic linkers. The luminescence properties are dependent on the coordination structures around the lanthanide ions and these characteristic coordination structures in network polymers lead to significant photophysical properties. In this section, photonic applications, photofunctional materials, and the photophysical properties of lanthanide coordination polymers are introduced.

4.1 Luminescent Thin films for organic electroluminescence (EL) devices

Luminescent lanthanide complexes are useful for the fabrication of organic EL devices. Various types of luminescent lanthanide complexes and luminescent polymers attached with lanthanie complexes have been reported. Figure 9 shows a schematic drawing of a typical organic EL device. The luminescence process in an emitting layer composed of lanthanide complexes is based on the excitation of π–π* transition bands. The recombination of an electron and a hole in an EL devices generally leads to the formation of excited singlet and triplet states of the ligands. The effective formation of an excited state in ligand molecules and effective energy transfer from the ligands to the lanthanide ions are key factors for organic EL

devices. Bettencout-Dias provided a review of lanthanide based emitting materials in the field of light-emitting diodes in 2007.[64]

However, effective organic EL devices based on the lanthanide coordination polymer have not yet been prepared, because lanthanide coordination polymers with network structures are not readily dissolved in general organic solvents. However, luminescent thin films containing lanthanide coordination polymers composed of Tb(III) ions, benzene-carboxylates, and 4,4'-bipyridines have been reported.[25] The coordination structure determined from single crystal XRD analysis was reported in Ref. 25. Wang and co-workers prepared thin firms by the spin-coating method with a methanol solution including $Tb(CH_3COO)_3$, benzene-carboxylates, and 4,4'-bipyridines. They suggested that the polymeric structure and co-existence are most likely responsible for the formation of a uniform and amorphous film from the solution. Thus, the key factor for the fabrication of thin films is the solubility of lanthanide coordination polymers with network structures.

4.2. Triboluminescent materials

In this section, we introduce the triboluminescence of lanthanide coordination polymers. Triboluminescence is the emission of light originating from mechanical stress on bulk solid materials.[65-67] At the present stage, various types of organic crystals, polymers, and metal complexes with triboluminescencent properties have been reported. While there have been extensive discussions on the origin of triboluminescence, some studies have indicated the contribution of the piezoelectric effect on the breaking of non-centrosymmetric bulk crystals.[68] Molecular crystals composed of Eu(III) complexes have also been studied for effective triboluminescence. Strongly luminescent lanthanide coordination polymer crystals with non-centrosymmetric structures are expected to exhibit efficient triboluminescence due to the generation of opposite electric charges on the opposing faces of cracks perpendicular to their polar axis.[68] We have reported brilliant triboluminescence from coordination polymer crystals with non-centrosymmetric structure, poly[3,3-bis(diphenylphosphoryl)-2,2-bipyridine][tris(hexafluoroacetyl-acetonate)]europium, $[Eu(hfa)_3(BIPYPO)]_n$ (Fig. 10).[69] The non-centrosymmetric lanthanide coordination polymer is composed of luminescent Eu(III) complexes with hfa and bidentate phosphine oxide ligands (BIPYPO). The coordination geometry of $[Eu(hfa)_3(BIPYPO)]_n$ is categorized as an asymmetric eight-coordinate square antiprism (8-SAP).

The nitrogen–phosphorus interaction provides a stable liner-type structure for $[Eu(hfa)_3(BIPYPO)]_n$. Two distinguishable structures of the BIPYPO ligand, assigned as BIPYPO A (S-form) and B (R-form), were observed in a $[Eu(hfa)_3(BIPYPO)]_n$ crystal, as illustrated in Fig. 11a. These independent BIPYPO A and B forms generate a non-centrosymmetric and chiral structure in poly-Eu-BIPYPO. Figure 11b shows the one-dimensional polymer chain in a columnar structure of the crystal. In this polymer chain structure, the Eu(III) ions are alternatively bridged by the BIPYPO A and B ligands. The distorted structure of the polymer chain results in a packing structure with the non-centrosymmetric Cc space group, which is suitable for piezoelectricity and triboluminescence.[65-67] The intense triboluminescence seems to originate from the non-centrosymmetric structure along with the polymer-like structure. The coordination polymer crystal exhibits remarkable triboluminescence because of their higher mechanical resistivity compared with that of typical triboluminescent lanthanide complexes.[68,70-72]

The emission quantum yield of the $[Eu(hfa)_3(BIPYPO)]_n$ crystal excited at 380 nm was as high as 61%, which is the highest value among those reported for triboluminescent Eu(III) crystals measured using a high-resolution optical system with a monochromator and photomultiplier. The high emission quantum yield is due to: (1) suppression of vibrational relaxation promoted by the low vibrational frequency hfa and phosphine oxide ligands,[73] (2) enhancement of radiative transition probability as a result of the asymmetric 8-SAP coordination structure,[74] and (3) efficient photosensitized energy transfer from the hfa ligands to the Eu(III) ions.

In $[Eu(hfa)_3(BIPYPO)]_n$ system, we also observed that the interligand charge transfer (ILCT) band via charge redistribution of the hfa ligands in the solid-state absorption spectrum of lanthanide coordination polymer crystal.[75] Eliseeva and Bünzli reported the effective photosensitized luminescence of a lanthanide complex through the ILCT band.[73] The relatively large emission quantum yield of the poly-Eu-BIPYPO crystals under UV light excitation may be due not only to the suppressed vibrational relaxation and enhancement of the radiative transition probability, but also to effective photosensitized luminescence through the ILCT band. The novel lanthanide coordination polymer, with a specific coordination structure of low vibrational frequency hfa and $[Eu(hfa)_3(BIPYPO)]_n$ coordination networks exhibits intense triboluminescence upon breaking, which is clearly observed even in daylight at room temperature (Fig. 10b). Here, we propose a molecular-level strategy and an ideal model for effective triboluminescent materials.

4.3 Thermo-sensor

In this section, the design of temperature-sensitive luminescent lanthanide coordination polymer is introduced. According to the historical study, Amao and co-workers reported the first temperature-sensitive film composed of Eu(III) complex and polymer matrix in 2003.[76-78] Khalil and coworkers demonstrated the high performance of thermo-sensing Eu(III) complex (temperature sensitivity: 4.42% $°C^{-1}$).[79] We have also reported a temperature-sensitive Tb(III) complex with hfa ligands. The effective temperature-sensing property is due to effective energy back transfer (EnBT) from the emission level of the Tb(III) ion to the excited triplet state of the hfa ligand.[80-82] EnBT is dependent on the energy barrier of the process; therefore, the emission intensity varies with temperature.

We here considered that the introduction of $Tb(hfa)_3$ unit into the coordination polymer framework would produce a thermo-sensitive lanthanide coordination polymer for high-temperature sinseing upon 100 °C. Secondly, we attempted to impart ratiometric temperature sensing ability using luminescent Eu(III) and Tb(III) ions in the coordination polymer to realize high thermosensing ability. Based on photophysical findings, $[Tb_{0.99}Eu_{0.01}(hfa)_3(dpbp)]_n$ was prepared as (Fig. 12b).[35] $[Tb_{0.99}Eu_{0.01}(hfa)_3(dpbp)]_n$ shows the characteristic emission bands at 543 and 613 nm are attributed to the 4f–4f transitions of Tb(III) ($^5D_4$–$^7F_5$) and Eu(III) ($^5D_0$–$^7F_2$), respectively. The emission intensity at 543 nm (Tb(III) ($^5D_4$–$^7F_5$) decreases dramatically with increasing temperature. In contrast, the emission intensity at 613 nm Eu(III) ($^5D_0$–$^7F_2$) increases slightly with the temperature.

Fig. 13 shows photographs that indicate the brilliant green, yellow, orange, and red photoluminescence of the $[Tb_{0.99}Eu_{0.01}(hfa)_3(dpbp)]_n$ sample under UV irradiation (365 nm) at 270, 300, 350, and 450 K, respectively. Color tuning of the coordination polymer in response to temperature change was achieved. $[Tb_{0.99}Eu_{0.01}(hfa)_3(dpbp)]_n$ has a higher temperature sensitivity (0.83% $°C^{-1}$) than $[Tb(hfa)_3(dpbp)]_n$ (0.64% $°C^{-1}$), which indicates that energy is transferred to both the excited triplet state of the hfa ligands (BEnT) and to the Eu(III) ion from the emission level of the Tb(III) ion.

The energy transfer efficiency from Tb(III) to Eu(III) ions increases with the temperature. The changes in the emission intensity ratio, I_{Eu}/I_{Tb}, values of 1.0 (300 K, yellow emission) and 8.7 (400 K, red emission) are stable and reproducible. $[Tb(hfa)_3(dpbp)]_n$ also exhibits red emission under UV irradiation, even at 500 K. Thus, an effective luminophore with a wide temperature sensing range of 200 to 500 K was successfully synthesized. In future, $[Tb_{0.99}Eu_{0.01}(hfa)_3(dpbp)]_n$ is expected to be a promising candidate for temperature-sensitive dyes, which are used for temperature distribution measurements of material surfaces such as an aerospace planes in wind tunnel experiments. Such lanthanide coordination polymers with thermosensing properties have the potential to open up new fields in supramolecular chemistry, polymer science, and molecular engineering.

4.5 Luminescent gels

Supramolecular polymers composed of metal ions and organic ligands have a number of interesting properties that make them attractive with respect to the development of stimuli-responsive polymers. Stimuli-responsive polymers provide an ideally dramstic change in properties upon application of an external stimulus, such as temperature, ionic strength, pH, electric, or magnetic field, or in the presence of chemical or biological analytes.

Rowan and Becka reported a supramolecular polyelectrolyte gels combined with lanthanide ions and bis-ligand monomers. The lanthanide polyelectrolyte gels shows thermo-, chemo-, and mechanical responses, as well as emission properties (Fig. 14).[83]

The bis-ligand is composed of a 2,6-bis-(benzimidazolyl)-4-hydrooxypyridine unit and a polyether chain. They also prepared mixed supramolecular polymers that contain lanthanide (Eu(III)) ions, and transition metal (Co(II) and Zn(II)) ions. The nature of the response was reported to be controlled by the combination of lanthanide and transition metal ions used.

4.6 Color and Brightness tuning in hetero-nuclear lanthanide coordination polymer

Lanthanide coordination polymers with terephthalate ligands, $[Ln_2(bdc)_3(H_2O)_4]_n$ (Ln = La–Tm (except Pm) plus Y),[84-87] provide microcrystalline powders by mixing aqueous solutions of lanthanide chloride and sodium terephthalate at room temperature, quantitatively. They present highly tunable luminescence properties.[86] Pollès, Bünzli, and Guillou have reported polynuclear heteronuclear lanthanide terephthalate coordination polymers, $[Ln_{2-2x}Ln'_{2x}(bdc)_3\text{-}(H_2O)_4]_n$, ($bdc^{2-}$:benzene-1,4-dicarboxylate) for color and brightness tuning.[88]

The spectroscopic and colorimetric properties of this family of compounds were investigated in detail. Pictures obtained under UV irradiation of heterotrimetallic $[Tb_{2x}Eu_{2y}La_{2-2x-2y}(bdc)_3(H_2O)_4]_n$ compounds with 2x and 2y between 0 and 2 are reported in Fig. 15. The trichromatic coordinates are located on the same straight line as the trichromatic coordinates of the heterobimetallic $[Tb_{2x}Eu_{2-2x}(bdc)_3(H_2O)_4]_n$ compounds. The emission color and brightness also depend on relative chemical composition of lanthanide ions.

The resulting data demonstrate that this series of compounds presents highly tunable luminescence properties. They have also reported here on a family of heterobimetallic and heterotrimetallic lanthanide-based coordination polymers in which brightness and color are tunable: (1) The best brightness was obtained for 20% doping in either Tb(III) or Eu(III) containing compounds. (2) The best color modulation was obtained for $0.7 \leq x \leq 1$ in the $[Eu_{2-2x}Tb_{2x}(bdc)_3(H_2O)_4]_n$ series. (3) The combined approach can be conducted by using heterotrinuclear coordination polymers.

$[La_{1.600}Dy_{0.352}Tb_{0.040}Eu_{0.008}(bdc)_3(H_2O)_4]_n$ also exhibits pale yellow luminescence under UV irradiation. Colorimetric measurements indicate that this luminescence is almost white (x = 0.40, y = 0.42).

4.6 Magneto-optical materials

Polynuclear metal complexes, where organic ligands are linked to metal clusters, is a type of metal coordination polymer. Polynuclear metal complexes exhibit characteristic chemical and physical properties such as catalytic activity,[89,90] magnetic coupling effects for single-molecular magnets,[91,92] and photosensitized luminescence between metal ions.[93,94] The molecular design of polynuclear metal complexes is expected to open up a new field of advanced molecular science.

Polynuclear metal complexes composed of lanthanide ions with 4f-orbitals have been recently synthesized and their characteristic physical properties have been investigated. Long et al. and Guo et al. have described the magnetically super-exchange coupling effect of binuclear Dy(III) complexes.[95,96] Piguet and coworkers have reported the enhancement of luminescence for polynuclear complexes by effective energy transfer from Cr(III) to Yb(III) ions.[97] We have also recently demonstrated a temperature-sensitive luminophore composed of Eu(III) and Tb(III) complexes.[35]

Specific metal-to-metal interactions in polynuclear lanthanide complexes induce active magnetic and photophysical behavior. We consider that the geometrical structures of polynuclear lanthanide complexes are related to their photomagnetic interactions with lanthanide ions. With respect to the magneto-optical behavior of lanthanide compounds, we have previously reported lanthanide inorganic materials, namely EuX nanocrystals (X = O, S, and Se) composed of Eu(II) and chalcogenide ions.[98-108] The inorganic Eu−X lattices exhibit a notable optical Faraday effect. The optical Faraday effect rotates the plane of polarized light in linear proportion to the component of the magnetic field in the direction of propagation. The Faraday effect is important for the construction of optical isolators for fiber-optic telecommunication systems.[109-120] The magneto-optical properties are induced in cubic Eu−X lattices. The Ln−O ordering bonds in polynuclear lanthanide complexes may provide novel aspects for the understanding of the optical Faraday effect.

Based on this concept, polynuclear Tb(III) complexes composed of Tb(III) ions and salicylate ligands, $[Tb_9(OH)_{10}(sal\text{-}Me)_{16}]^-$, were prepared (Fig. 16).[121] All polynuclear Tb(III) complexes were composed of nine Tb(III) ions, sixteen salicylate ligands, ten OH parts, and one nitrate anion. The nonanuclear Tb(III) complexes were characterized using single crystal XRD analysis. The Tb(III) complexes have characteristic sandglass-shaped structures composed of nine Tb(III) ions, sixteen salicylate ligands, eight bridged μ_3-OH^- parts, and two μ_4-OH^- parts. All Tb(III) ions are surrounded by eight

oxygens, which is the typical coordination number of lanthanide(III) complexes. The selected distances and angles are directly linked to the coordination geometry. On the basis of the crystal data, calculations on the shape factor S were performed to estimate the degree of distortion for an ideal coordination structure. The S value is given by

$$S = min\sqrt{\frac{1}{m}\sum_i^m(\delta_i - \theta_i)^2} \quad (1)$$

where m, δ_i, and θ_i are the number of possible edges (m = 18 in this study), the observed dihedral angle between planes along the edge, and the dihedral angle for the ideal structure, respectively. The coordination geometry of the typical lanthanide complex has two characteristic geometries around the Tb(III) ions: the trigonal dodecahedron (8-TDH) with a D2d point group and the square antiprism (8-SAP) with a D4d point group, as shown in Fig. 17. The S values of the central Tb ions in $[Tb_9(OH)_{10}(sal\text{-}Me)_{16}]^-$ were determined as 1.34° for 8-SAP and 14.45° for 8-TDH. From these results, the central Tb ion was identified as 8-SAP with a small S value.

In contrast, the S values of the eight Tb(III) ions of $[Tb_9(OH)_{10}(sal\text{-}Me)_{16}]^-$ in the upper and lower units were found to be ca. 16.84° for 8-SAP and ca. 11.64° for 8-TDH. The eight Tb(III) ions in the upper and lower square units were classified as having the 8-TDH structure.

The optical Faraday rotation of polynuclear Tb(III) complexes (Fig. 18) was observed in the visible region, which is the first such observation for a single lanthanide complex. We have also successfully estimated the enhanced magnetic exchange interaction from room temperature electron paramagnetic resonance (EPR) measurements. The polynuclear Tb(III) complexes are much larger than those of Tb(III) oxide glass. Polynuclear lanthanide complexes composed of Ln−O lattices are expected to lead to novel Faraday materials with magneto-optical properties.

4.7 Nano-sized luminescent materials

The characteristic tight-stacking structures of lanthanide coordination polymers generally lead to formation of insoluble compounds, as microsized particles, in water and organic solvents. The insoluble microsized particles prevent the preparation of transparent materials for optical use due to multiple light scattering in the UV-Vis region. Nanosized lanthanide coordination polymer particles without multiple light scattering could be applied as future optical and luminescent materials. Buildup and breakdown methods have been reported for the preparation of organo molecule nanoparticles. For example, Kasai et al. described a reprecipitation method for the formation of perylene nanocrystals.[122] In addition, Jeon et al. have presented a laser ablation method in liquid media for the preparation of organic dyes and pigment nanoparticles.[123]

Lin and co-workers have reported on the luminescent organo-nanorods containing Eu(III) or Tb(III) ions.[124] The nanorods were prepared by stirring an optically transparent microemulsion of $GdCl_3$ and bis(methylammonium)benzene-1,4-dicarboxylate (BCD) (in a 2:3 molar ratio) in a cationic cetyltrimethylammoniumbromide (CTAB)/isooctane/1-hexanol/water system for 2 h. The morphologies and sizes of the nanorods were influenced by the water/surfactant molar ratio w, of the microemulsion systems. For example, nanorods with 40 nm diameters and 100-125 nm long were obtained with w = 5 and a Gd(III) concentration of 50 mM. The particle size was also affected by the reactant concentration and ratio. A decrease in the concentration of reactants or a deviation of the metal-to-ligand molar ratio from 2:3 typically resulted in a decrease of the particle size (**Fig. 19**). They have also successfully synthesized luminescent nanorods using Eu(III) or Tb(III) dopants. Mixing 5 mol% $EuNO_3$ or $TbNO_3$ during the syntheses resulted in nanorods with similar sizes and morphologies, and with compositions of $Gd_{0.95}(BDC)_{1.5}(H_2O)_2$:$Eu_{0.05}$ and $Gd_{0.95}(BDC)_{1.5}(H_2O)_2$:$Tb_{0.05}$. However, the quantitative emission properties of these complexes have not been reported.

Daiguebonne et al. have prepared nanoparticles of luminescent lanthanide terephthalate coordination polymers, $[Ln_2(C_8H_4O_4)_3(H_2O)_4]_n$,[125] of which the Tb(III)-containing compounds exhibit large quantum yields of up to 43%. Polyvinylpyrrolidone nanoparticles doped with $[Ln_2(C_8H_4O_4)_3(H_2O)_4]_n$ (Ln = Eu, Tb, and Er) were also synthesized and characterized.The encapsulation of the coordination polymers results in somewhat reduced luminescence intensities and lifetimes, but the nanoparticles can be dispersed in water and remain unchanged in this medium for more than 20 h.

Kimizuka and coworkers reported the self-assembly of amorphous nanoparticles of supramolecular coordination polymer networks from nucleotides and lanthanide ions in water.[58] Those self-assembly nanosystem shows efficient energy transfer from the nucleobase to the lanthanide ions and excellent performance as contrast enhancing agents for magnetic resonance imaging (MRI). Preparations of lanthanide coordination nanoparticles assisted with surface stabilizers have been also reported by Daiguebonne and co-workers.[125]

We have focused on the characteristic formation of organo-nanoparticles using a micelle technique in liquid media, such as the preparation of nanoscale organic compounds. The preparation of polystyrene nanoparticles using micelle techniques have been reported in the field of polymer science.[126] The micelle sizes are also controlled by the concentration and molecular structure of the organosurfactants in water as the medium.[127, 128] Nanoparticles composed of lanthanide coordination polymers with strong luminescence properties were prepared based on the micelle technique.[129] The luminescent nanoparticles were obtained by the polymerization of $Eu(hfa)_3(H_2O)_2$ with dpbp as a linker ligand in micelles under water. The particle size was controlled using sodium lauryl sulfate (SDS) and n-octyltrimethylammonium bromide (TMOA) in water. A scheme for the preparation of luminescent nanoparticles using the micelle technique is given in Fig. 20.

The structure of the resultant nanoparticles was characterized using electrospray ionization-mass spectrometry (ESI-MS) and XRD measurements. The sizes of the prepared A, B, and C micelles (Fig. 20) were measured using the dynamic light scattering (DLS) technique. The formation of nanoparticles (average size: 66 nm) was successfully achieved using the micelle reaction technique in water.

The thermal decomposition temperature of the lanthanide coordination nanoparticles and bulk powders of lanthanide coordination polymers were estimated to be 301 and 302 °C, respectively. Nanoparticles composed of $[Eu(hfa)_3(dpbp)]_n$ had effective thermal stability based on the characteristic rigid structure of $[Eu(hfa)_3(dpbp)]_n$ with CH/π and CH/F interactions.[9] The lanthanide coordination nanoparticles may be useful for high temperature industrial molding and soldering processes. The emission lifetime of the nanoparticles was 0.91±0.01 ms, which is the same as that for the bulk powders (0.91±0.01 ms). Thus, it is considered that the emission properties of the nanoparticles

composed of lanthanide coordination polymers are the same as those of the bulk lanthanide coordination polymers.

Lanthanide coordination nanoparticles can also be used to improve optical transmittance because they decrease multiple light scattering in the UV-Vis region. The use of strongly luminescent nanoparticles composed of lanthanide coordination polymers may lead to the development of new applications for future luminescent

5. Energy transfer in lanthanide coordination polymers

5.1 Energy transfer between Tb(III) and Eu(III)

Photophysical studies on the energy transfer from Tb(III) ions to Eu(III) ions have been conducted using mono- and di-nuclear lanthanide complexes in homogeneous organic and aqueous media.[130,131] Kinetic analysis of the photophysical properties of solid-state coordination polymers can directly reveal novel aspects in the fields of solid-state photochemistry.

$[Tb,Eu(hfa)_3(dpbp)]_n$ complexes were prepared with various Tb/Eu ratios (1, 10, 250, 500, 750) and the thermosensitive performance and energy transfer efficiency were investigated. The structures of the prepared lanthanide coordination polymers were analyzed using powder XRD analyses. The observed peaks are attributed to the geometrical structure of $[Tb,Eu(hfa)_3(dpbp)]_n$. of the XRD peaks for the $[Tb,Eu(hfa)_3(dpbp)]_n$ complexes correspond well with those for $[Eu(hfa)_3(dpbp)]_n$,[132] which indicates that the geometric structures of $[Tb,Eu(hfa)_3(dpbp)]_n$ are the same as that of $[Eu(hfa)_3(dpbp)]_n$.] Based on the crystal data for $[Eu(hfa)_3(dpbp)]_n$.], the distances between Eu(III) ions located within inter- and intra-polymer chains have been found to be 11.4 Å and 13.6 Å, respectively (Fig. 21). The critical distance for energy transfer between lanthanide ions has been calculated to be approximately 12 Å.[132] With respect to the distance for energy transfer, we consider that inter-polymer chain energy transfer would be dominant because it is shorter (11.4 Å). The distances between Ln(III) ions in the solid-state polymer matrix is considered to make effective energy transfer between Ln(III) ions available.

The temperature dependence of the ratio of luminescent intensities of Tb(III) at 543 nm and Eu(III) ions at 615 nm (I_{Eu}/I_{Tb}) in $[Tb,Eu(hfa)_3(dpbp)]_n$ with various Tb/Eu ratios were measured in the temperature range of 100-350 K to estimate the energy transfer efficiency between Tb(III) ions and Eu(III) ions in a solid-state polymer matrix, and the results are shown in Fig. 22. I_{Eu}/I_{Tb} is dependent on the ion ratio of Tb(III) and Eu(III) ions.

It is considered that the emission spectral ratio for various concentrations of $[Tb,Eu(hfa)_3(dpbp)]_n$ and the temperature-dependence of the emission spectra are directly linked to the energy transfer process between Tb(III) and Eu(III) ions. The energy transfer efficiency from Tb(III) to Eu(III) ions ($\eta_{Tb\text{-}Eu}$) is estimated using equation (2):[133]

$$\eta_{Tb-Eu} = 1 - \frac{\tau_{obs}}{\tau_{Tb}} \quad (2)$$

where τ_{obs} and τ_{Tb} are the emission lifetimes of $[Tb,Eu(hfa)_3(dpbp)]_n$ and $[Tb(hfa)_3(dpbp)]_n$, respectively. The lifetime measurements were monitored at the *4f-4f* transition bands of the Tb(III) ion for $^5D_4$-$^7F_6$ (545 nm) and $^5D_4$-$^7F_5$ (488 nm). The energy transfer efficiencies between Tb(III) and Eu(III) ions at 100 K for the various Tb/Eu ratios were equivalent and approximately zero. The photophysical phenomenon is similar to that in previous study on the energy transfer between Tb(III) and Eu(III) ions in the solid-state.[134] According to measurements at 300 K, the energy transfer efficiencies $\eta_{Tb\text{-}Eu}$, are 99, 65, 7.4, and 8.2% for Tb/Eu = 1, 10, 250, and 500, respectively. These results indicate that $\eta_{Tb\text{-}Eu}$ is dependent on the concentration of the Eu(III) ions as the energy transfer acceptor.[135]

The thermosensitive performance and energy transfer efficiency from Tb(III) ions to Eu(III) ions were determined to be dependent on the Tb/Eu ratio in the lanthanide coordination polymers. In particular, characteristic energy transfer properties of lanthanide coordination polymers composed of Tb(III) ions and a small amount of Eu(III) ions (e.g., Tb/Eu = 750) have been observed (η_{Tb-Eu} showed negative value (33%)). We are now attempting to analyze these unusual photophysical properties using magneto-optical measurements on $[Tb,Ln(hfa)_3(dpbp)]_n$ (Ln = Nd, Sm, Eu, Gd, Dy, and Yb) complexes. For solid-state polymers, the authors also consider that the π-orbitals in the ligands can influence the thermosensing properties. Such studies are thus expected to provide novel aspects on the energy transfer mechanisms in solid-state lanthanide coordination polymers.

6. Conclusions

Lanthanide coordination polymers with characteristic photophysical properties are expected to be applied in the field of photonic science. In this review, we have introduced the characteristics of lanthanide ion emissions, the formation of lanthanide coordination polymers, and their thermostability. In luminescent thin films for future organic EL devices, triboluminescent materials, thermosensors for material surfaces, luminescent gels from supramolecular systems, magneto-optical materials for photonic telecommunication systems, and luminescent nanoparticles composed of lanthanide coordination polymers for future photonic materials.

The characteristic energy transfer efficiency from Tb(III) to Eu(III) ions in solid state lanthanide coordination polymers was presented in section 5. The photonic properties of lanthanide coordination polymers include a combination of the characteristic properties of typical organic, metal complexes, and inorganic photonic materials. From these reasons, the luminescent materials constructed lanthanide coordination polymers are independent of typical organo-dyes, luminescent metal complexes, and inorganic-phosphors.

Lanthanide coordination polymers are expected to be useful for applications in energy conversion systems (e.g., applied materials for silicon solar cells) [136] and as luminescent paints for security sensors.[13,137-139] The authors envisage that further research and development on luminescent lanthanide polymers could realize new optical devices in the near future. Lanthanide coordination polymers are expected to open up new fields of

research in materials science, coordination chemistry, polymer science, and advanced photonic engineering.

Acknowledgements

The author is very grateful to emeritus Prof. S. Yanagida (Osaka University), Prof. Y. Wada (Tokyo Institute of Technology), Prof. T. Kawai, Prof. T. Nakashima, Dr. J. Yuasa (Nara Institute of Science and Technology), Prof. N. Nakashima (Osaka City University), Prof. T. Yamanaka (Osaka University), Prof. K. Murakoshi, Prof. M. Kato, Prof. H. Ito, Prof. Y. Hinatsu, Prof. H. Koizumi, Dr. A. Kobayashi, Dr. T. Seki, Dr. Y. Doi (Hokkaido University), Prof. K. Tanaka, Prof. K. Fujita (Kyoto University), Prof. P. O'Brien (University of Manchester), Prof. T. Asahi (Ehime University), Dr. K. Nakamura (Chiba University), Dr. T. Nakagawa (Yokohama National University), Dr. Y. Kuramochi (Kitasato University), Dr. T. Harada (Shimane University), Prof. K. Fushimi, Dr. Y. Kitagawa (Hokkaido University) for collaboration, measurements, and helpful comments. I would also like to thank the members of the Laboratory of Molecular Process Engineering at Osaka University, Laboratory for Photonic Molecular Science at Nara Institute of Science and Technology, and Laboratory of Advanced Materials Chemistry at Hokkaido University.

This work was partly supported by Grants-in-Aid for Scientific Research on Innovative Areas of "New Polymeric Materials Based on Element-Blocks (No. 2401)" (No. 24102012) of the Ministry of Education, Culture, Sports, Science and Technology (MEXT), Japan.

Abbreviations

MOF	metal-organic framework
Ln-MOF	metal-organic framework composed lanathnide ions
Eu(III)	Europium(III) ion
Tb(III)	Terbium(III) ion
hfa	hexafluoroacetylacetone
dpb	1,4-bis(diphenylphosphoryl)benzene
dpbp	4,4'-bis(diphenylphosphoryl)biphenyl
dppcz	3,6-bis(diphenylphosphoryl)-9-phenylcarbazole
biphepo	1,1'-Biphenyl-2,2¢-diylbis(diphenylphosphine oxide
bipypo	1,1'-Biphenyl-2,2¢-diylbis(dipyridylphosphine oxide
sal-Me	methyl salytylate
bdc	benzenedicarboxylic acid
TGA	Thermo gravitic analysis
DSC	Differential scaning calorymetor
8-SAP	eitht coordinated square antiprism
ILCT	Interligand Charge Transfer
EnT	Energy transfer
BEnT	Energy back transfer
sal-Me	methylsalythylate
EPR	electron paramagnetic resonance
BCD	bis(methylammonium)benzene-1,4-dicarboxylate
CTAB	cetyltrimethylammoniumbromide
SDS	sodium lauryl sulphate
TMOA	n-Octyltrimethylammonium Bromide
ESI-MS	Electro-spray mass spectrometry
XRD	X-ray diffraction measurement
DLS	dynamic light scattering measurements

References

1 D. F. Shriver and P. W. Atkins, *Inorganic Chemistry third edition*, OXFORD university press, 1999, 320.
2 Y. Hasegawa, Y. Wada and S. Yanagida, *J. Photochem. Photobio. C Photochem. Rev.,* 2004, **5**, 183.
3 G. Blassse and B. C. Grabmaier, *Luminescent Materials*, Springger-Verlag, Berlin Heidelberg, 1994.
4 A. Thirumurugan, S. K. Pati, M. A. Greenc and S. Natarajan, *J. Mater. Chem.,* 2003, **13**, 2937.
5 C. Daiguebonne, N. Kerbellec, O. Guillou, J.-C. G. Büzli, F. Gumy, L. Catala, T. Mallah, N. Audebrand, Y. Geraut, K. Bernot and G. Calvez, *Inorg. Chem.,* 2008, **47***,* 3700.
6 K. Binnemans, *Chem. Rev.,* 2009, **109**, 4283.
7 C. Marchal, Y. Filinchuk, X.-Y. Chen, D. Imbert, and M. Mazzanti, *Chem. Eur. J*., 2009, **15**, 5273.
8 T. M. Reineke, M. Eddaoudi, M. Fehr, D.Kelley, and O. M. Yaghi, *J. Am. Chem. Soc*., 1999, **121**, 1651–1657.
9 J. Rocha, L. D. Carlos, F. A. A. Paza, and D. Ananias, *Chem. Soc. Rev.*, 2011, **40**, 926–940.
10 Y.-Q. Sun, J. Zhanga, and G.-Y. Yang, *Chem. Commun.*, 2006, 4700–4702.
11 Z.-H. Zhang, T. Okamura, Y. Hasegawa, H. Kawaguchi, L.-Y. Kong, W.-Y. Sun, and N. Ueyama, *Inorg. Chem.,* 2005, **44**, 6219-6227.
12 D. T. Lill, A. Bettencourt-Dias, and C. L. Cahill, *Inorg. Chem.*, 2007, **46**, 3960-3965.
13 K. A. White, D. A. Chengelis, K. A. Gogick, J. Stehman, N. L. Rosi, and S. Petoud, *J. Am. Chem. Soc.,* 2009, **131**, 18069.
14 P. Mahata, and S. Natarajan, *Inorg. Chem.*, 2007, **46**, 1250–1258.
15 X. Feng, J. Zhao, B. Liu, L. Wang, S. Ng, G. Zhang, J. Wang, X. Shi, and Y. Liu, *Cryst. Grow. & Desi.,* 2010, **10**, 1399–1408.
16 Z. He, C. He, E.-Q. Gao, Z.-M. Wang, X.-F. Yang, C.-S. Liao, and C.-H. Yan, *Inorg. Chem.,* 2003, **42**, 2206-2208.
17 C. Serre, F. Pelle, N. Gardant, and G. Ferey, *Chem. Mater.*, 2004, **16**, 1177-1182.
18 T. R. Cook, Y.-R. Zheng, and P. J. Stang, *Chem. Rev.*, 2013, **113**,734-777.
19 C. Seidel, C. Lorbeer, J. Cybińska, A.-V. Mudring, and U. Ruschewitz, *Inorg. Chem*., 2012, **51**, 4679−4688.
20 B. D. Chandler, J. O. Yu, D. T. Cramb, and G. K. H. Shimizu, *Chem. Mater.*, 2007, **19**, 4467–4473.
21 W. Liu, T. Jiao, Y. Li, Q. Liu, M. Tan, H. Wang, and L. Wang, *J. Am. Chem. Soc.*, 2004, **126**, 2280–2281.
22 L. Pan, K. M. Adams, H. E. Hernandez, X. Wang, C. Zheng, Y. Hattori, and K. Kaneko, *J. Am. Chem. Soc.*, 2003, **125**, 3062–3067.
23 B. V. Harbuzaru, A. Corma, F. Rey, P. Atienzar, J. L. Jord, H. Garc, D. Ananias, and L. D. Carlos, J. Rocha, *Angew. Chem. Int. Ed.*. 2008, **47**, 1080 –1083.
24 J. Rocha, L. D. Carlos, F. A. A. Paza, and D. Ananias, *Chem. Soc. Rev.*, 2011, **40**, 926–940.
25 C. Seward, N-X. Hub, and S. Wang, *J. Chem. Soc., Dalton Trans*., 2001, 134-137.
26 C. Daiguebonne, N. Kerbellec, O. Guillou, J.-C. Bünzli, F. Gumy, L. Catala, T. Mallah, N. Audebrand, Y. Gérault, K. Bernot, and G. Calvez, *Inorg. Chem.,* 2008, **47**, 3700-3708.
27 H. Zhang, L. Zhou, J. Wei, Z. Li, P. Lin, and S. Du, *J. Mater.*

Chem., 2012, **22**, 21210-21217.
28 A. de Bettencourt-Dias, *Inorg. Chem.* 2005, **44**, 2734-2741.
29 J. Yang, Q. Yue, G-D Li, J-J Cao, G-H Li, and J-S. Chen, *Inorg. Chem.*, 2006, **45**, 2857-2865.
30 Z. Wang, C.-M. Jin, T. Shao, Y.-Z.. Li, K.-L. Zhang, H.-T. Zhang, and X.-Z. You, *Inorg. Chem. Comm.,* 2002, **5**, 642–648
31 Y.-Q. Suna, and G.-Y. Yang, *Dalton Trans.*, 2007, 3771–3781.
32 Y. Huang, B. Wu, D. Yuan , Y. Xu, F Jiang, and M. Hong, *Inorg. Chem.,* 2007, **46**, 1171-1176.
33 H.-S. Wang, B. Zhao, B. Zhai, W. Shi, P. Cheng, D.-Z. Liao, and S.-P. Yan, *Cryst. Grow. & Desi.,* 2007, **7**, 1851-1857.
34 K. Miyata, T. Ohba, A. Kobayashi, M. Kato, T. Nakanishi, K. Fushimi, and Y. Hasegawa, *ChemPlusChem,* 2012, **77***,* 277.
35 K. Miyata, Y. Konno, T. Nakanishi, A. Kobayashi, M. Kato, K. Fushimi, and Y. Hasegawa, *Angew. Chem. Int. Ed*. 2013, **52**, 6413.
36 Y. Hasegawa, K. Murakoshi, Y. Wada, S. Yanagida, J. Kim, N. Nakashima, and T. Yamanaka, *Chem. Phys. Lett.* 1996, **248**, 8.
37 Y. Hasegawa, Y. Kimura, K. Murakoshi, Y. Wada, T. Yamanaka, J. Kim, N. Nakashima, and S. Yanagida, *J. Phys. Chem.* 1996, **100**, 10201.
38 Y. Hasegawa, M. Iwamuro, K. Murakoshi, Y. Wada, R. Arakawa, T. Yamanaka, N. Nakashima and S. Yanagida, *Bull. Chem. Soc. Jpn.,* 1998, **71,** 2573-2581.
39 S. Yanagida, Y. Hasegawa, K. Murakoshi, Y. Wada, N. Nakashima and T. Yanamaka, *Coord. Chem. Rev.,* 1998, **171**, 461-480.
40 Y. Hasegawa, T. Ohkubo, K. Sogabe, Y. Kawamura, Y. Wada, N. Nakashima and S. Yanagida, *Angew. Chem. Int. Ed.,* 2000, **39**, 357-360.
41 Y. Wada, T. Okubo, M. Ryo, T. Nakazawa, Y. Hasegawa and S. Yanagida, *J. Am. Chem. Soc.*, 2000, **122**, 8583-8584.
42 S. Yanagida, Y. Hasegawa and Y. Wada, *J. Lumin.*, 2000, **87-89**, 995-998.
43 M. Ryo, Y. Wada, T. Okubo, T. Nakazawa, Y. Hasegawa and S. Yanagida, *J. Mater. Chem.,* 2002, **12**, 1748-1753.
44 M. Ryo, Y. Wada, T. Okubo, Y. Hasegawa and S. Yanagida, *J. Phys. Chem. B,* 2003, **107**, 11302-11306.
45 Y. Hasegawa, M. Yamamuro, Y. Wada, N. Kanehisa, M. Kai, and S. Yanagida, *J. Phys. Chem. A,* 2003, **107**, 1697.
46 K. Nakamura, Y. Hasegawa, H. Kawai, N. Yasuda, N. Kanehisa, Y. Kai, T. Nagamura, S. Yanagida, and Y. Wada, *J. Phys. Chem. A.* 2007, **111***,* 3029.
47 Y. Hasegawa, Y. Wada, S. Yanagida, H. Kawai, N. Yasuda and T. Nagamura, *Appl. Phys. Lett.,* 2003, **83**, 3599-3601.
48 Y. Hasegawa, H. Kawai, K. Nakamura, N. Yasuda, Y. Wada and S. Yanagida, *J. Alloy Compd.,* 2006, **408-412**, 669.
49 K. Nakamura*,* Y. Hasegawa*,* H. Kawai, N. Yasuda*,* Y. Wada and S. Yanagida*, J. Alloy Compd.,* 2006, **408-412**, 771.
50 T. Harada, Y. Hasegawa, Y. Nakano, M. Fujiki, M. Naito, T. Wada, Y. Inoue and T. Kawai*, J. Alloy. Compd.,* 2009, **488**, 599-602.
51 K. Miyata, Y. Hasegawa, Y. Kuramochi, T. Nakagawa, T. Yokoo and T. Kawai*, Eur. J. Inorg. Chem.,* 2009,.
52 T. Harada, Y. Hasegawa, Y. Nakano, M. Fujiki, M. Naito and T. Kawai, *Inorg. Chem.,* 2009, **48**, 11242-11250.
53 S. Kishimoto, T. Nakagawa and T. Kawai and Y. Hasegawa, *Bull Chem. Soc. Jpn.,* 2011, **82**, 148-154.
54 K. Miyata, T. Nakagawa, R. Kawakami, Y. Kita, K. Sugimoto, T. Nakashima, T. Harada, T. Kawai, and Y. Hasegawa, *Chem. Eur. J.* 2011, **17***,* 521.
55 Y. Kuramochi, T. Kawai, and Y. Hasegawa, *Dalton Trans.,* 2012, **41**, 6634-6640.
56 K. Miyata, T. Nakanishi, K. Fushimi, and Y. Hasegawa, *J. Photochem. Photobio. A*, 2012, **235**, 35-39.
57 Y. Hasegawa, T. Ohkubo, T. Nakanishi, A. Kobayashi, M. Kato, T. Seki, H. Ito and K. Fushimi, *Eur. J. Inorg. Chem.,* 2013, 5911-5918.
58 M. Murata, C. Adachi, Y. Katayama, M. Hashizume, and N. Kimizuka, *J. Am. Chem. Soc.*, 2009, **131**, 2151–2158.
59 F. Marchetti, C. Pettinari, A. Pizzabiocca, A. A. Drozdov, S. I. Troyanov, C. O. Zhuravlev, S. N. Semenov, Y. A. Belousov, and I. G. Timokhin, *Inorg. Chim. Acta,* 2010, **363**, 4038.
60 C. Wang, Y. Xing, Z. Li, J. Li, X. Zeng, M. Ge, and S. Niu, *J. Mol. Struct.* 2009, **931**, 76.
61 A. R. Ramya, D. Sharma, S. Natarajan, and M. L. P. Reddy, *Inorg. Chem.,* 2012, **51**, 8818-8826..
62 G. R. Desiraju, and T. Steiner in *The Weak Hydrogen Bond in Structural Chemistry and Biology*, Oxford Univ. Press, Oxford, 1999.
63 P. Slavíček, and M. Fárník, Phys. Chem. Chem. Phys. 2011, **13**, 12123 –12137.
64 A. Bettencourt-Dias, Dalton Trans., 2007, 2229–2241.
65 G. Wiedemann, and F. Schmidt, *Ann. Phys.* (Leipzig) 1895, **54**, 604.
66 A. J. Walton, *Adv. Phys.* 1977, **26**, 887.
67 J. I. Zink, *Accounts Chem. Res.* 1978*,* **11**, 289.
68 X.-F. Chen, X.-H. Zhu, Y.-H. Xu, S. Shanmuga Sundararaj, S. ztürk, H.-K. Fun, J. Ma, and X.-Z. You, *J. Mater. Chem.* 1999, **9**, 2919.
69 Y. Hasegawa, R. Hieda, K. Miyata, T. Nakagawa and T. Kawai, *Eur. J. Inorg. Chem.* 2011, 4978.
70 P. C. R. Soares-Santos, H. I. S. Nogueira, F. A. Almeida Paz, R. A. Sá Ferreira, L. D. Carlos, J. Klinowski, and T. Trindade, *Eur. J. Inorg. Chem.* 2003, 3609.
71 B. V. Bukvetskii, A. G. Mirochnik, P. A. Zhikhareva, and V. E. Karasev, *J. Struct. Chem*. 2006, **47***,* 575.
72 X.-L. Li, Y. Zheng, J.-L. Zuo, Y. Song, and X.-Z. You, *Polyhedron* 2007, **26**, 5257.
73 S. V. Eliseeva, O. V. Kotova, F. Gumy, S. N. Semenov, V. G. Kessler, L. S. Lepnev, J.-C. G. Bünzli, and N. P. Kuzmina, *J. Phys. Chem. A*, 2008, **112**, 3614–3626.
74 L. N. Puntus, K. A. Lyssenko, M. Y. Antipin, and J.-C. G. Bünzli, *Inorg. Chem*., 2008, **47**, 11095–11107.
75 Y. Hasegawa, R. Hieda, T. Nakagawa, and T. Kawai, *Helv. Chim. Acta*, 2009, **92**, 2238–2248.
76 S. Shindo, *Low-speed Wind Tunnel Testing Technique*, Corona, Tokyo, 1992, Chap. 1.
77 *Proceedings of MOSAIC International Workshop*, November 10 – 11, 2003, Tokyo, Japan.
78 M. Mitsuishi, S. Kikuchi, T. Miyashita, and Y. Amao, *J. Mater. Chem.* 2003, **13**, 2875.
79 G. E. Khalil, K. Lau, G. D. Phelan, B. Carlson, M. Gouterman, J. B. Callis, and L. R. Dalton, *Rev. Sci. Instrum.* 2004, **75**, 192.
80 S. Katagiri, Y. Hasegawa, Y. Wada, and S. Yanagida, *Chem. Lett*. 2004, **33**, 1438.
81 S. Katagiri, Y. Hasegawa, Y. Wada, K. Mitsuo and S. Yanagida, *J. Alloy Compd.,* 2006, **408-412***,* 809.
82 S. Katagiri, Y. Tsukahara, Y. Hasegawa and Y. Wada, *Bull. Chem. Soc. Jpn.*, 2007, **80***,* 1492.
83 S, J. Rowan, and J. B. Becka, *Faraday Discuss.*, 2005, **128**, 43–53.
84 T. M. Reneike, M. Eddaoudi, M. Fehr, D. Kelley, and O. M. Yaghi, *J. Am. Chem. Soc.,* 1999, **121**, 1651.
85 C. Daiguebonne, N. Kerbellec, O. Guillou, J. C. G. Bünzli, F. Gumy, L. Catala, T. Mallah, N. Audebrand, Y. Gérault, K. Bernot, and G. Calvez, *Inorg. Chem.*, 2008, **47**, 3700.
86 N. Kerbellec, D. Kustaryono, V. Haquin, M. Etienne, C.

Daiguebonne, and O. Guillou, *Inorg. Chem.* 2009, **48**, 2837.
87 V. Haquin, F. Gumy, C. Daiguebonne, J. C. G. Bünzli, and O. Guillou, *Eur. J. Inorg. Chem.* 2009, 491.
88 V. Haquin, M. Etienne, C. Daiguebonne, S. Freslon, G. Calvez, K. Bernot, L. Le Pollès, S. E. Ashbrook, M. R. Mitchell, J.-C. Bünzli, S. V. Eliseeva, and O. Guillou, *Eur. J. Inorg. Chem.*, 2013, 3464–3476.
89 Y. Shimazaki, T. Nagano, H. Takesue, B. H. Ye, F. Tani, and Y. Naruta, *Angew. Chem., Int. Ed.,* 2004, **43**, 98−100.
90 Z. Hou, Y. Luo, and J.-X. Li, *Organomet. Chem.*, 2006, **691**, 3114−3121.
91 S. Ohkoshi, K. Imoto, Y. Tsunobuchi, S. Takano, and H. Tokoro, *Nature,* 2011, **3**, 564−569.
92 P. H. Lin, T. J. Burchell, R. Clérac, and M. Murugesu, *Angew. Chem., Int. Ed.*, 2008, **47**, 8848−8851.
93 Y. Li, S. Ren, Q. Liu, J. Ma, X. Chen, H. Zhu, and Y. Dong, *Inorg. Chem.*, 2012, **51**, 9629−9635.
94 S. Torelli, D. Imbert, M. Cantuel, G. Bernardinelli, S. Delahaye, A. Hauser, J.-C. G. Bünzli, and C. Piguet, *Chem. Eur. J.*, 2004, **10**, 3228−3242.
95 J. Long, F. Habib, P. Lin, I. Korobkov, G. Enright, L. Ungur, W. Wernsdorfer, J. F. Chibotaru, and M. Murugesu, *J. Am. Chem. Soc.*, 2011, **133**, 5319−5328.
96 Y. Guo, G. Xu, W. Wernsdorfer, L. Ungur, Y. Guo, J. Tang, H. Zhang, L. F. Chibotaru, and A. K. Powell, *J. Am. Chem. Soc.,* 2011, **133**, 11948−11951.
97 L. Aboshyan-Sorgo, H. Nozary, A. Aebischer, J.-C. G. Bünzli, P. Morgantini, K. R. Kittilstved, A. Hauser, S. V. Eliseeva, S. Petoud, and C. Piguet, *J. Am. Chem. Soc.*, 2012, **134**, 12675−12684.
98 Y. Hasegawa, M. Maeda, T. Nakanishi, Y. Doi, Y. Hinatsu, K. Fujita, K. Tanaka, H. Koizumi, and K. Fushimi, *J. Am. Chem. Soc.,* 2013, **135**, 2659−2666.
99 T. Nakanishi, M. Maeda, A. Kawashima, K. Fujita, K. Tanaka, K. Fushimi, and Y. Hasegawa, *J. Alloys Compd.*, 2013, **562**, 123−127.
100 A. Kawashima, T. Nakanishi, T. Shibayama, S. Watanabe,K. Fujita, K. Tanaka, H. Koizumi, K. Fushimi, and Y. Hasegawa, *Chem. Eur. J.*, 2013, **19**, 14438−14445.
101 Y. Hasegawa, S. Thongchant, Y. Wada, H. Tanaka, T. Kawai, T. Sakata, H. Mori, and S. Yanagida, *Angew. Chem., Int. Ed.*, 2002, **41**, 2073−2075.
102 S. Thongchant, Y. Hasegawa, Y. Wada, and S. Yanagida, *J. Phys. Chem. B*, 2003, **107**, 2193−2196.
103 Y. Hasegawa, M. A. Afzaal, P. O'Brien, Y. Wada, and S. Yanagida, *Chem. Commun.* 2005, 242−243.
104 T. Kataoka, Y. Tsukahara, Y. Hasegawa, and Y. Wada, *Chem. Commun.*, 2005, 6038−6040.
105 Y. Hasegawa, Y. Okada, T. Kataoka, T. Sakata, H. Mori, and Y. Wada, *J. Phys. Chem. B,* 2006, **110**, 9008−9011.
106 Y. Hasegawa, T. Adachi, A. Tanaka, M. Afzaal, P. O'Brien, Y. Doi, Y. Hinatsu, K. Fujita, K. Tanaka, and T. Kawai, *J. Am. Chem. Soc.*, 2008, **130**, 5710−5715.
107 A. Tanaka, H. Kamikubo, Y. Doi, Y. Hinatsu, M. Kataoka, T. Kawai, and Y. Hasegawa, *Chem. Mater.*, 2010, **22**, 1776−1781.
108 A. Tanaka, H. Kamikubo, M. Kataoka, Y. Hasegawa, and T. Kawai, *Langmuir,* 2011, **27**, 104−108.
109 J. K. urdyna, *J. Appl. Phys.*, 1988, **64**, R29−R64.
110 J. A. Gaj, J. Ginter, R. R. Galazka, *Phys. Status Solidi B*, 1978, **89**, 655−662.
111 H. Ohno, A. Shen, F. Matsukura, A. Oiwa, A. Endo, S. Katsumoto, and Y. Iye, *Appl. Phys. Lett.*, 1996, **69**, 363−365.
112 Y. Ohno, D. K. Young, B. Beschten, F. Matsukura, H. Ohno, and D. D. Awschalom, *Nature*, 1999, **402**, 790−792.
113 T. Jungwirth, W. A. Atkinson, B. H. Lee, and A. H. MacDonald, *Phys. Rev. B*, 1999, **59**, 9818−9821.
114 Y. Wang, N. Herron, K. Moller, and T. Bein, *Solid State Commun.*, 1991, **77**, 33− 38.
115 D. J. Norris, N. Yao, and F. T. Charnock, and T. A. Kennedy, *Nano Lett.,* 2001, 1, 3−7.
116 Y. W. Jun, Y. Y. Jung, and J. Cheon, *J. Am. Chem. Soc.,* 2002, **124**, 615−619.
117 C. A. Stowell, R. J. Wiacek, A. E. Saunders, and B. A. Korgel, *Nano Lett.*, 2003, **3**, 1441.
118 N. S. Norberg, K. R. Kittilstved, J. E. Amonette, R. K. Kukkadapu, D. A. Schwartz, and D. R. Gamelin, *J. Am. Chem. Soc.*, 2004, **126**, 9387−9398.
119 S. C. Erwin, L. Zu, M. I. Haftel, A. L. Efros, T. A. Kennedy, and D. J. Norris, *Nature*, 2005, **436**, 91−94.
120 R. Beaulac, P. I. Archer, X. Liu, S. Lee, G. M. Salley, M. Dobrowolska, J. K. Furdyna, and D. R. Gamelin, *Nano Lett.*, 2008, **8**, 1197−1201.
121 T. Nakanishi, Y. Suzuki, Y. Doi, T. Seki, H. Koizumi, K. Fushimi, K. Fujita, Y. Hinatsu, H. Ito, K. Tanaka and Y. Hasegawa, *Inorg. Chem.,* 2014, **53**, 7635-7641.
122 H. Kasai, H. Oikawa, S. Okada, and H. Nakanishi, *Bull. Chem. Soc. Jpn.,* 1998, **71**, 2597.
123 H. G. Jeon, T. Sugiyama, H. Masuhara, and T. Asahi, *Jpn.J. Appl. Phys.,* 2007, **46**, L733.
124 W. J. Rieter, K. M. L. Taylor, H. An, W. Lin, and W. Lin, *J. Am. Chem. Soc.,* 2006, **128**, 9024-9025.
125 C. Daiguebonne, N. Kerbellec, O. Guillou, J.-C. Bünzli, F. Gumy, L. Catala, T.Mallah, Nathalie Audebrand, Y. Gérault, K. Bernot, and G. Calvez, *Inorg. Chem.,* 2008, **47**, 3700-3708.
126 S. S. Atik, and J. K. Thomas, *J. Am. Chem. Soc.,* 1981, **103**, 4279.
127 M. Antonietti, S. Lohmann, and C. V. Niel, *Macromolecules,* 1992, **25**, 1139.
128 M. Boutonnet, J. Kizling, P. Stenius, and G. Maire, *Colloids Surfaces,* 1982, **5**, 209.
129 H. Onodera, T. Nakanishi, K. Fushimi, Y. Hasegawa, *Bull. Chem. Soc. Jpn.,* 2014, in press.
130 J.-F. Lemonnier,§ L. Gu**é**en**é**e, C**.** Beuchat, T. A. Wesolowski, P. Mukherjee, D. H. Waldeck, K. A. Gogick, S. Petoud, and C. Piguet, *J. Am. Chem. Soc.*. 2011, **133**, 16219–162134.
131 A. M. Funk, P. H. Fries, P. Harvey, A. M. Kenwright, and D. Parker, *J. Phys. Chem. A,* 2013, **117**, 905–917.
132 Y. Hasegawa, K. Murakoshi, Y. Wada, T. Yamanaka, J. Kim, N. Nakashima and S. Yanagida*, Chem. Phys. Lett.* 260, **173-177** (1996).
133 C. Piguet, J.-C. G. Bnzli, G. Bernardinelli, G. Hopfgartner, and A. F. Williams, *J. Am. Chem. Soc.*, 1993, **115**, 8197.
134 C. D. S. Brites, P. P. Lima, N. J. O. Silva, A. Millán, V. S. Amaral, F. Palacio, and L. D. Carlos, *Adv. Mater.* 2010, **22,** 4499–504.
135 Y. Hirai, T.Nakanishi, K. Miyata, K. Fushimi, Y. Hasegawa, *Mater. Lett.*, 2014, **130,** 91-93.
136 H. Kataoka, T. Kitano, T. Takizawa, Y. Hirai, T. Nakanishi, and Y. Hasegawa, *J. Alloys Compd* . 2014, **601**, 293–297.
137 T. Harada, H. Tsumatori, K. Nishiyama, J. Yuasa, Y. Hasegawa, and T. Kawai,, *Inorg. Chem.,* 2012, **51**, 6476-6485.
138 T. Harada, Y. Hasegawa, Y. Nakano, M. Fujiki, M. Naito and T. Kawai, *Inorg. Chem.,* 2009, **48**, 11242-11250.
139 J. Yuasa, T. Ohno, K. Miyata, H. Tsumatori, Y. Hasegawa, T. Kawai, *J. Am. Chem. Soc.,* 2011, **133**, 9892–9902.
140 Onodera, T. Nakanishi ,K. Fushimi , and Y. Hasegawa, *Bull. Chem. Soc. Jpn.* in press.

Figure captions

Fig. 1 Energy diagrams of lanthanide(III) ions. Numerical values in figures show wavelength (μm) of the emission bands.

Fig. 2 Structures of a) Ln-MOF and b) Ln coordination polymer composed of Ln(III) ions and organic ligands.

Fig. 3. Various types of linker ligands for formation of lanthanide coordination polymers.

Fig. 4. Structural images of lanthanide coordination polymers. Reference from a) A. Daiguebonne [26]. Copyright (2008) American Chemical Society, b) A. de Bettencourt-Dias[28] Copyright (2005) American Chemical Society, c) C. Seward[25] Copyright (2001) The Royal Society of Chemistry, and d) N. Kimizuka[58] Copyright (2009) American Chemical Society.

Fig. 5. Lanthanide coordination polymers composed of three-dimensional network structures. Reference from T. Nakanishi and Y. Hasegawa[34]. Copyright (2012) Wiley-VCH Verlag GmbH& Co. KGaA, Weinheim.

Fig. 6 Coordination structures with of CH/F and CH/π interactions of a) $[Eu(hfa)_3(dpb)]$, b) $[Eu(hfa)_3(dpbp)]$, and c) $[Eu(hfa)_3(dppcz)]$. Reference from T. Nakanishi and Y. Hasegawa[34] Copyright (2012) Wiley-VCH Verlag GmbH& Co. KGaA, Weinheim.

Fig. 7. Left: Diffuse-reflectance absorption spectra of $[Eu(hfa)_3(dpb)]_n$ (blue line), $[Eu(hfa)_3(dpbp)]_n$ (red line), $[Eu(hfa)_3(dppcz)]_n$ (orange line), and $[Eu(hfa)_3(H_2O)_2]$ (dot line) in the solid state. The absorption bands at 310 nm are attributed to a π–π* transition of the hfa ligands. The small bands at 465 nm are assigned to the $^7F_0$–$^5D_2$ transition in the EuIII ion. Right: Emission spectra of $[Eu(hfa)_3(dpbp)]_n$, $[Eu(hfa)_3(dppcz)]_n$, and $[Eu(hfa)_3(dpb)]_n$ in the solid state. Excitation wavelength is 465 nm. The spectra were normalized with respect to the magnetic dipole transition ($^5D_0$–$^7F_1$). Inset: Photographs of (a) previously reported EuIII complex, $[Eu(hfa)_3(biphepo)]$ and (b) $[Eu(hfa)_3(dpbp)]_n$ after heating at 280 °C for 10 min under UV irradiation (365 nm). Reference from T. Nakanishi and Y. Hasegawa[34]. Copyright 2012 Wiley-VCH Verlag GmbH& Co. KGaA, Weinheim.

Fig. 8 Layered structure constructed by helical lanthanide-carboxylate chain of $[Ln_4(m\text{-}BDC)_6(H_2O)_4(DMF)]\cdot(H2O)2(DMF)$ Reference from S. Du. [27] Copyright (2012) The Royal Society od Chemistry.

Fig. 9 Schematic drawing of organic EL devices. Emitting layer is containing luminescent lanthanide complexes or luminescent polymers attached with lanthanide complexes. HTL: hole transport layer. ETL: electron transport layer.

Fig. 10 a) Chemical structure of $[Eu(hfa)_3(BIPYPO)]_n$. b) Observed sequence-picture images of triboluminescence from poly-Eu-BIPYPO powder upon pushing with a black stickat ambient temperature and in daylight. Reference from Y. Hasegawa[69]. Copyright (2011) Wiley-VCH Verlag GmbH& Co. KGaA, Weinheim.

Fig. 11 a) Chemical structure of$[Eu(hfa)_3(BIPYPO)]_n$. b) (a–h) Observed sequence-picture images of triboluminescence from $[Eu(hfa)_3(BIPYPO)]_n$ powder upon pushing with a black stick at ambient temperature and in daylight. c) (a) A- and B-type structures of BIPYPO molecules in poly-Eu-BIPYPO crystals. (b) Packing structure of poly-Eu-BIPYPO crystals. Reference from Y. Hasegawa[69]. Copyright (2011) Wiley-VCH Verlag GmbH& Co. KGaA, Weinheim.

Fig. 12 a) Energy transfer processes of the Eu(III) and Tb(III) coordination polymer (EnT: energy transfer, EnBT: energy back transfer, Em: emission). b) Chemical structure of $[Ln(hfa)_3(dpbp)]_n$ (Ln=Eu, Tb). Reference from T. Nakanishi and Y. Hasegawa[35]. Copyright (2013) Wiley-VCH Verlag GmbH& Co. KGaA, Weinheim.

Fig.13. Color pictures of [Tb0.99Eu0.01(hfa)3(dpbp)]n under UV (365 nm) irradiation, which show (a) 250K (brilliant green), (b) 270K (yellow), (c) 300K (light yellow), (d) 350K (orange), and (e) 450K (red). Reference from T. Nakanishi and Y. Hasegawa[35]. Copyright (2013) Wiley-VCH Verlag GmbH& Co. KGaA, Weinheim.

Fig. 14. Schematic representation of the formation of a metallo supramolecular gel using a combination of lanthanide and transition metal ions mixed with monomer. Reference from S. J. Rowan[85]. Copyright (2005) The Royal Society of Chemistry.

Fig.15 Pictures obtained under UV irradiation of heterotrimetallic $[Tb_{2x}Eu_{2y}La_{2-2x-2y}(bdc)_3(H_2O)_4]_n$ compounds with 2x and 2y between 0 and 2. Reference from O. Guillou [88] Copyright 2013 Wiley-VCH Verlag GmbH & Co. KGaA, Weinheim.

Fig. 16. Chemical structure and ORTEP drawing of $[Tb_9(OH)_{10}(sal\text{-}Me)_{16}]^-$. Reference from T. Nakanishi and Y. Hasegawa [121]. Copyright (2014) American Chemical Society.

Fig. 17. Coordination structures of eight-coordinated squareantiprism (8-SAP) and eight-coordinated trigonal dodecahedron (8-TDH).

Fig. 18. Image of Faraday rotation of polarized light using polynucler Tb(III) complex. Reference from T. Nakanishi and Y. Hasegawa [121]. Copyright (2014) American Chemical Society.

Fig. 19. SEM images of $Gd(BDC)_{1.5}(H_2O)_2$ (1) nanorods synthesized with w) 5 (left) and w) 10 (right). Reference from W. J. Rieter [124]. Copyright (2006) American Chemical Society.

Fig. 20. Preparation scheme of luminescent nanoparticles composed of lanthanide coordination polymers, $[Eu(hfa)_3(dpbp)]_n$, using micelle techniques in water. Reference from T. Nakanishi and Y. Hasegawa [140] Copyright (2014) The Chemical Society of Japan.

Fig. 21 Crystal structures of $[Eu(hfa)_3(dpbp)]_n$ focused on the distances between Eu(III) ions in inter- and intra-polymer chains. Reference from T. Nakanishi and Y. Hasegawa [135]. Copyright (2014) Elsevier B.V.

Fig. 22 (a)Temperature dependence of relative emission intensities (I_{Eu}/I_{Tb}, ▲: Tb/Eu = 10, ●: Tb/Eu = 250, ■: Tb/Eu = 500 and ▼: Tb/Eu = 750). Reference from T. Nakanishi and Y. Hasegawa [135]. Copyright (2014) Elsevier B.V.

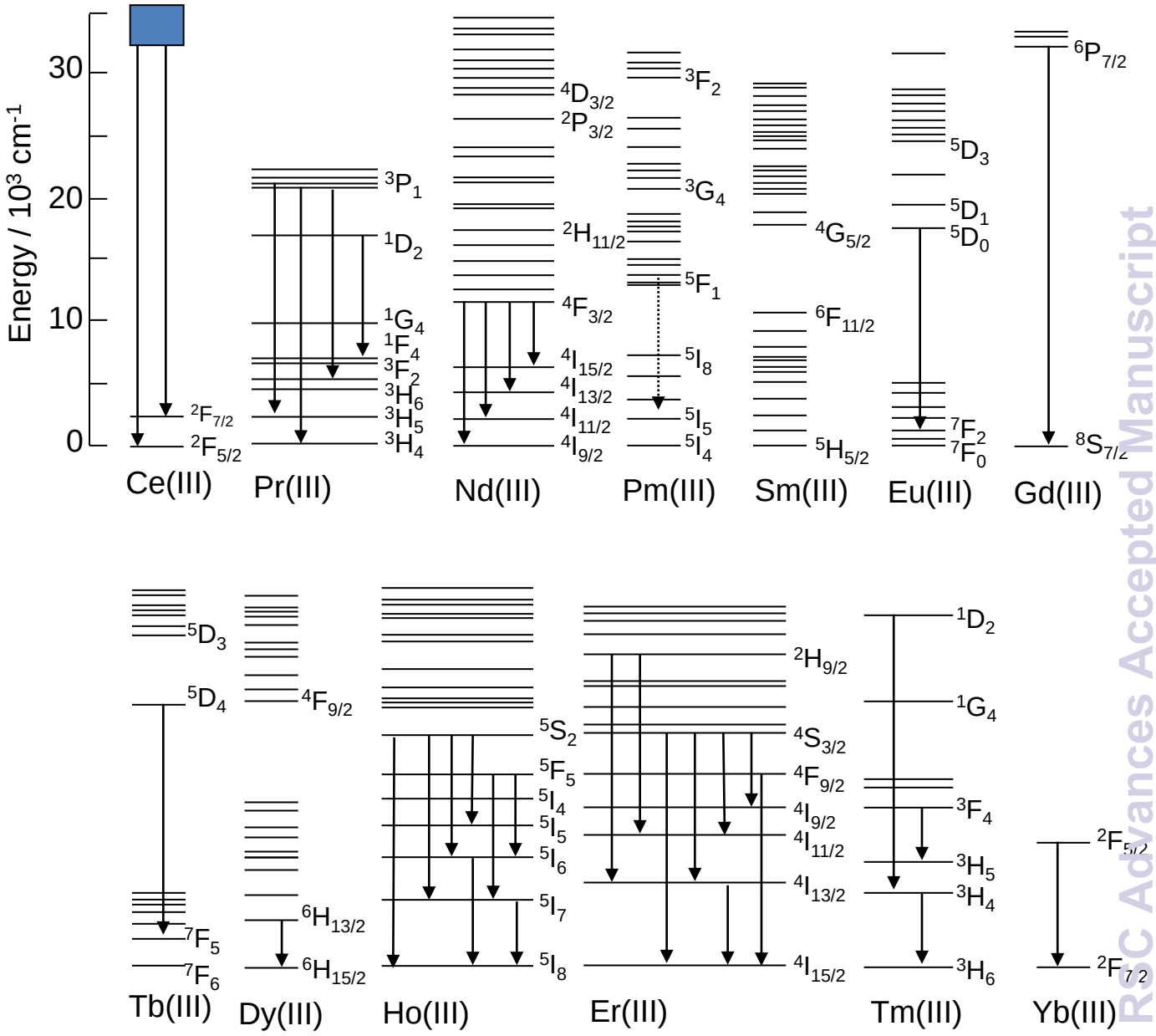

Y. Hasegawa and T. Nakanishi, Fig.2

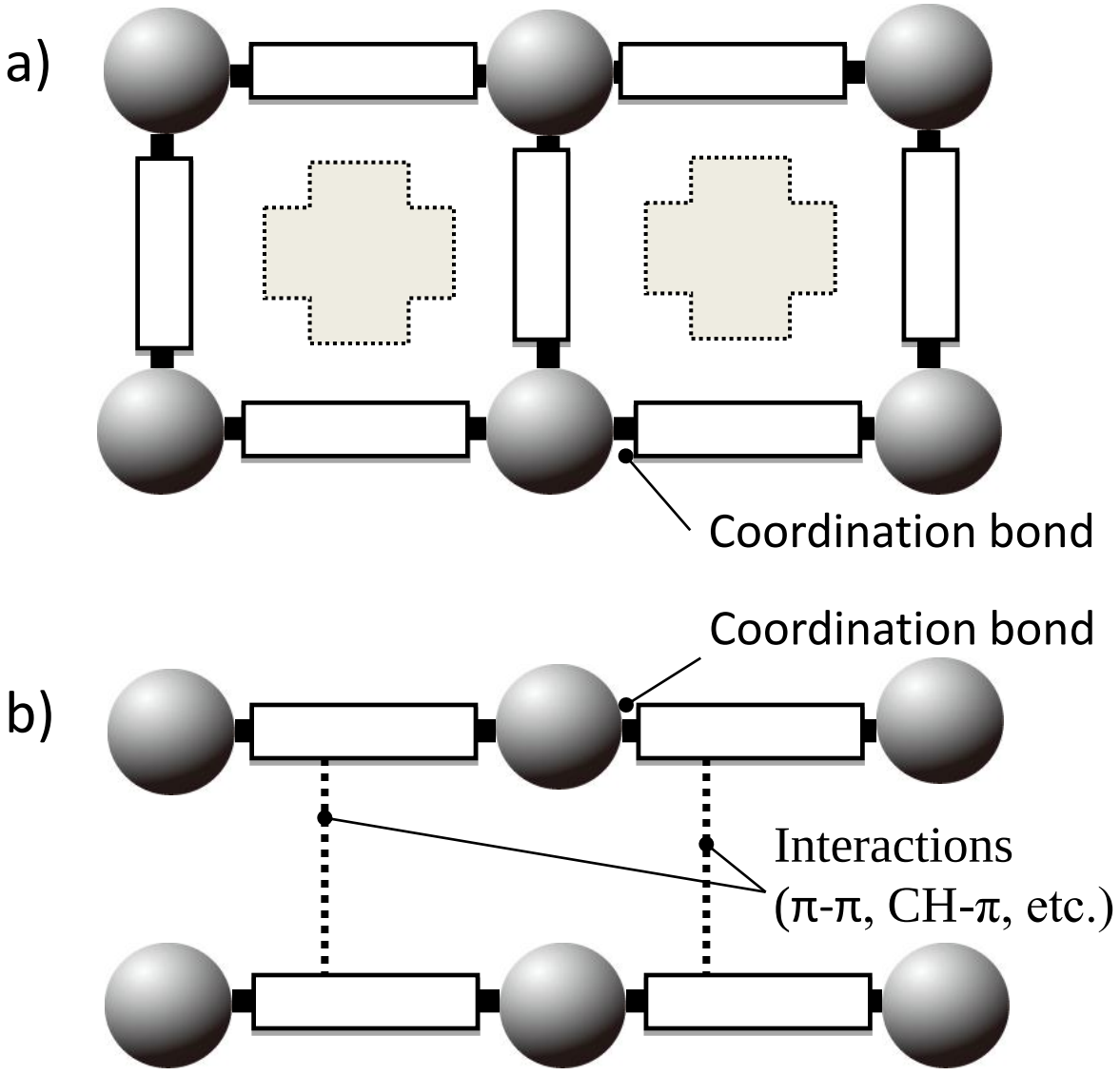

Y. Hasegawa and T. Nakanishi, Fig.3

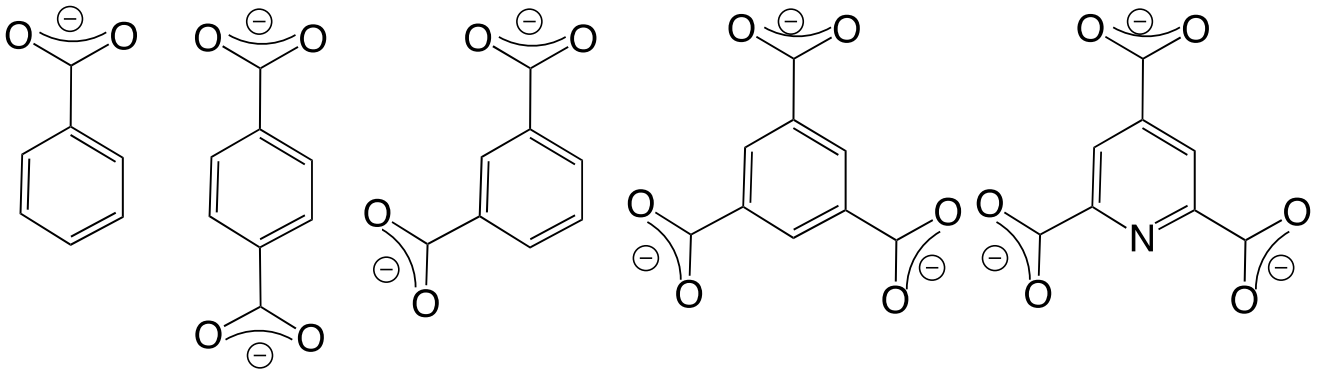

a b c d e

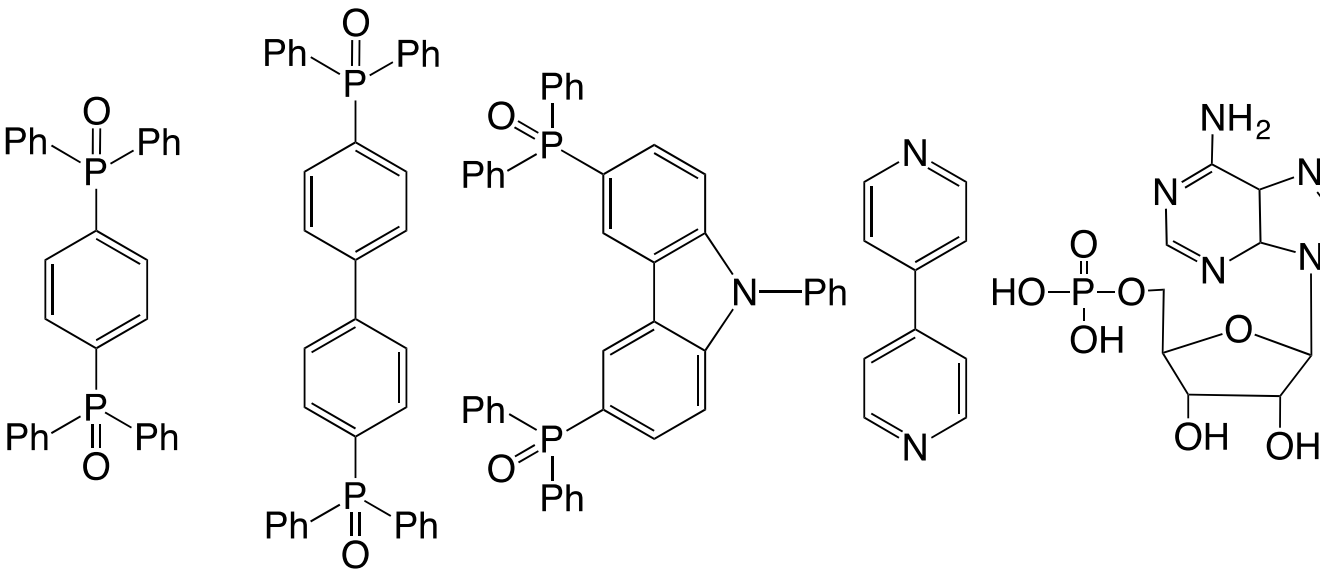

f g h i j

Y. Hasegawa and T. Nakanishi, Fig.4

a)

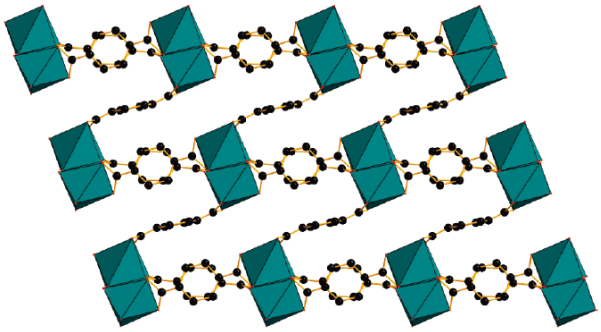

b)

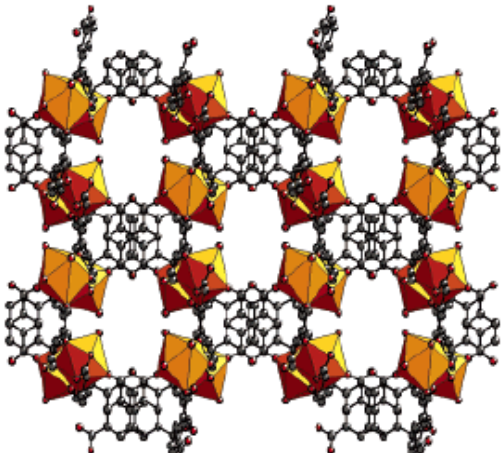

c)

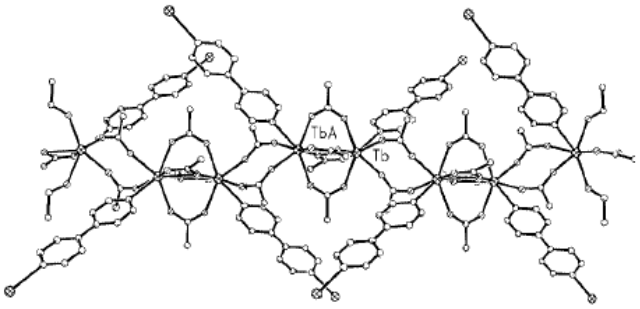

d)

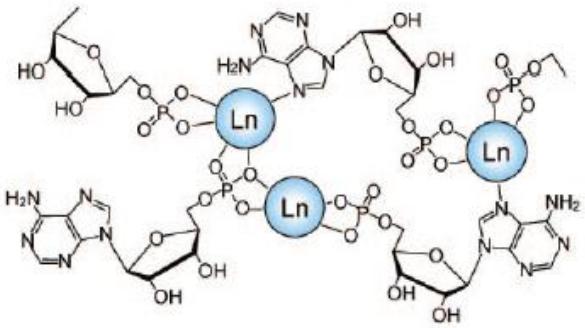

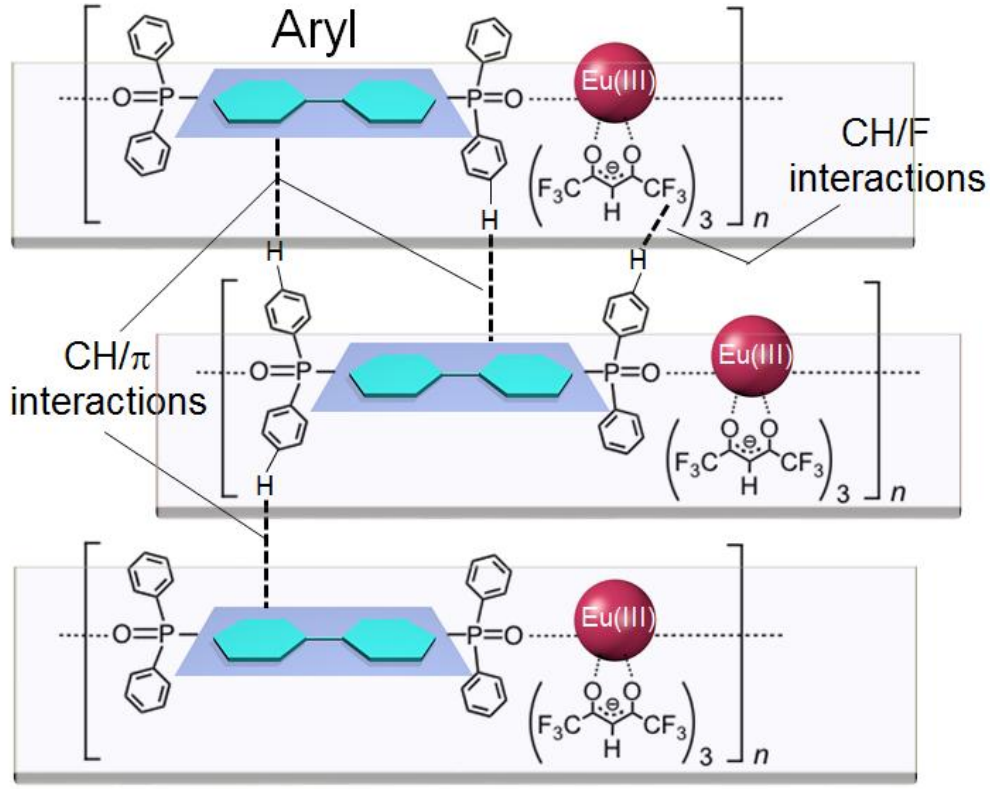

Y. Hasegawa and T. Nakanishi, Fig.6

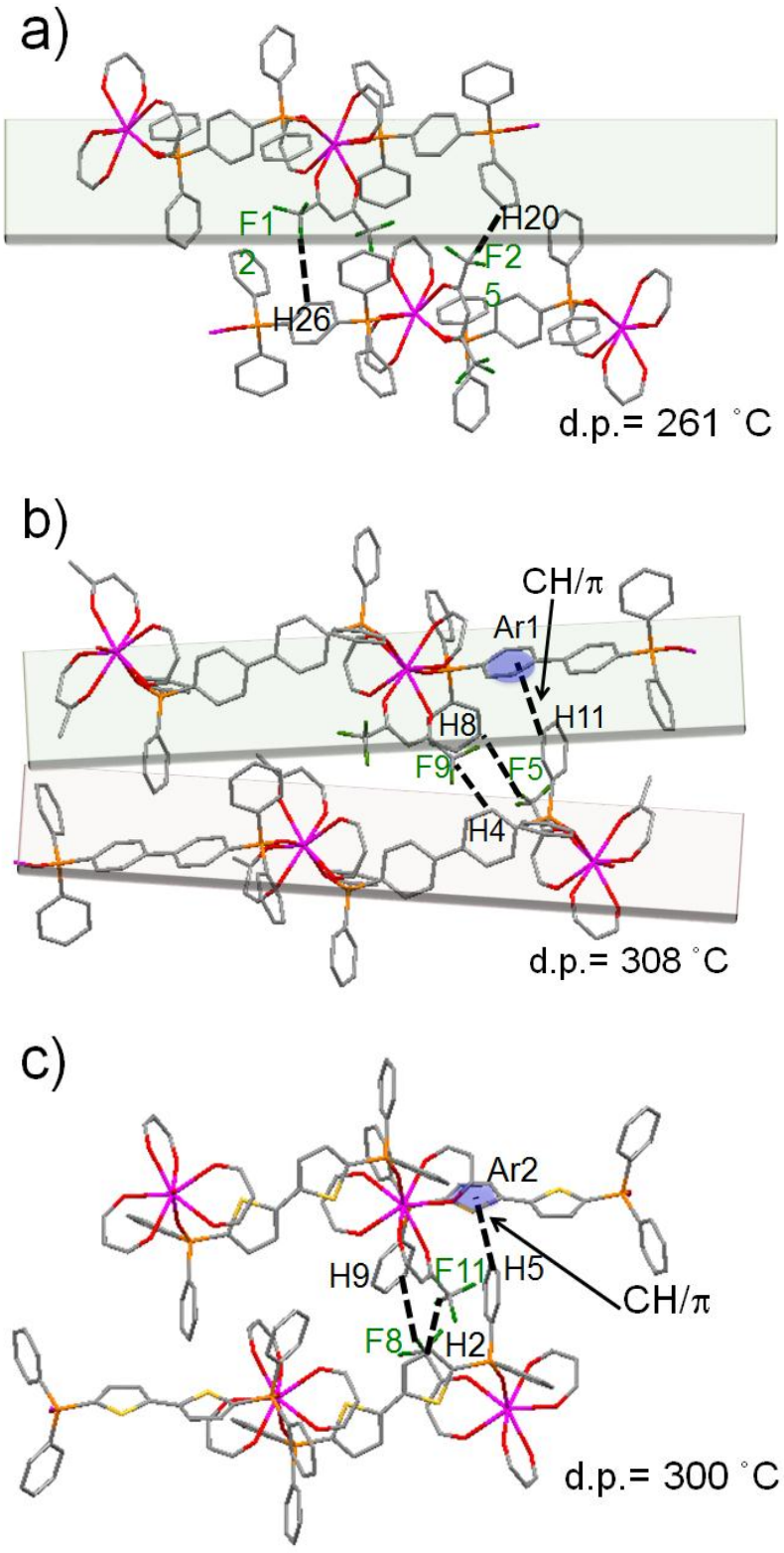

Y. Hasegawa and T. Nakanishi, Fig.7

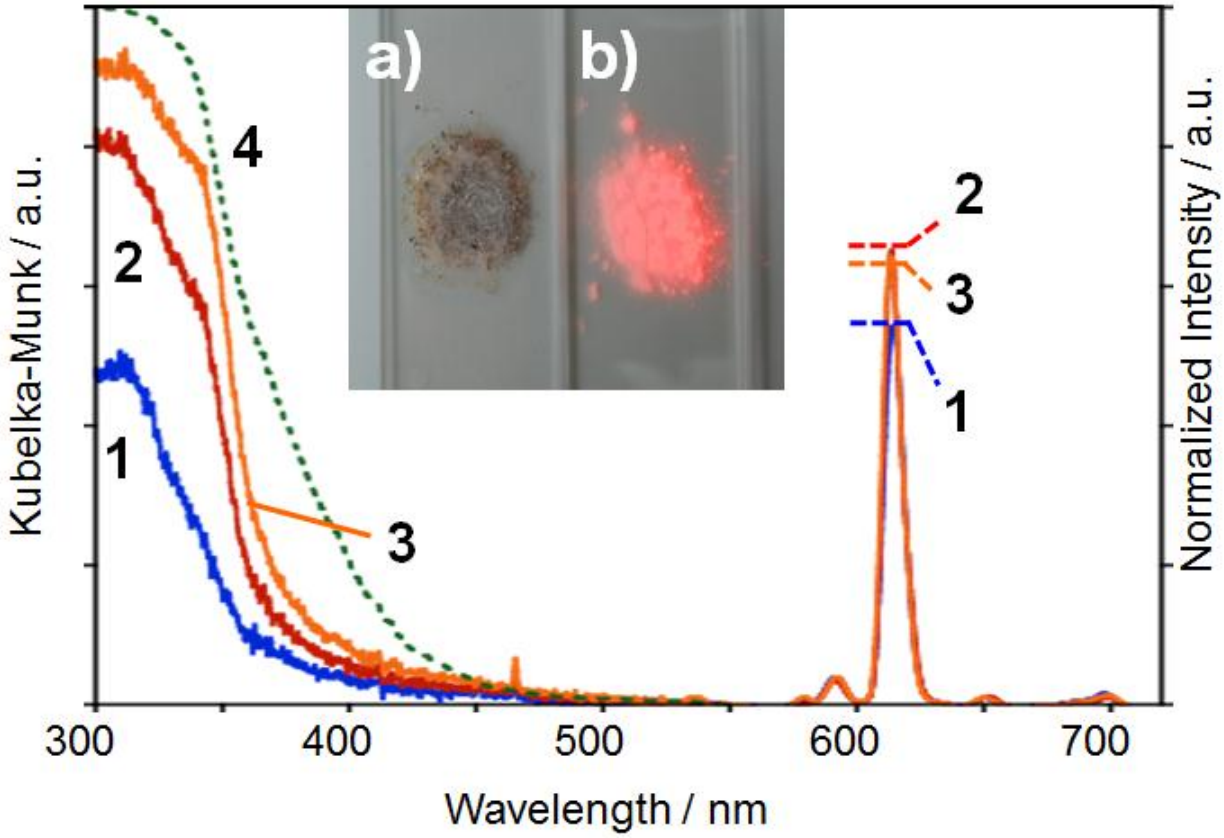

T. Hasegawa and T. Nakanishi, Fig.8

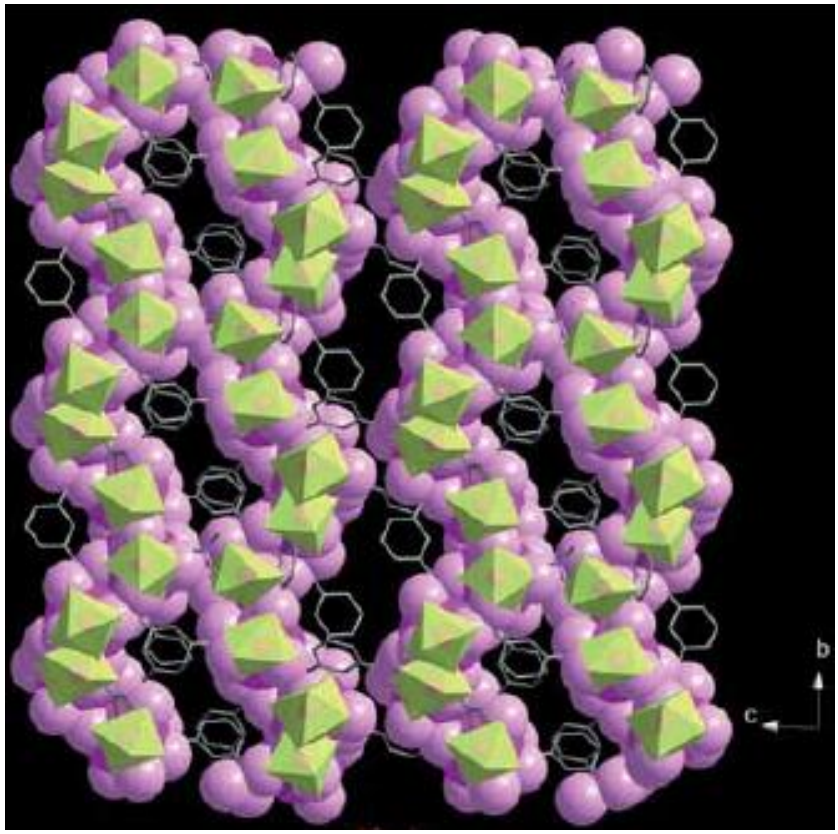

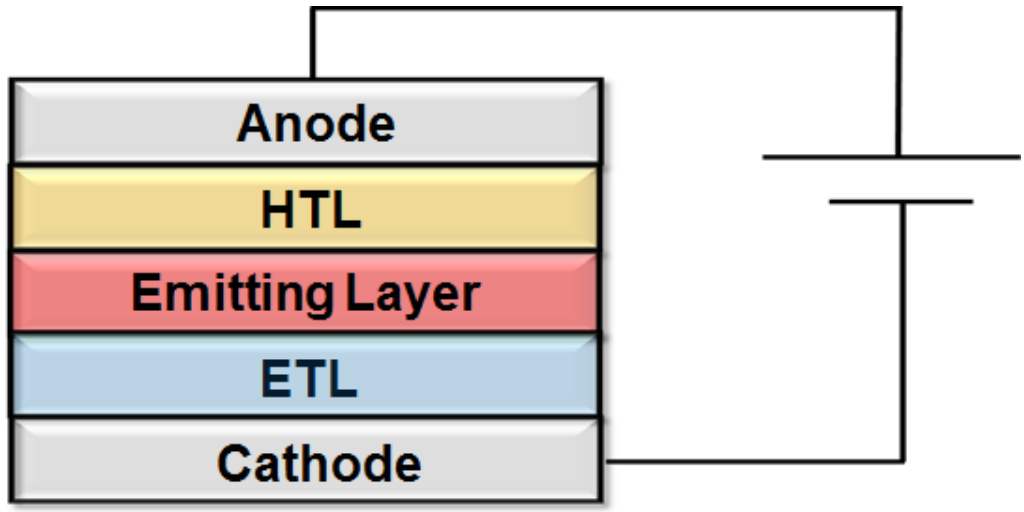

Y. Hasegawa and T. Nakanishi, Fig.10

(a)

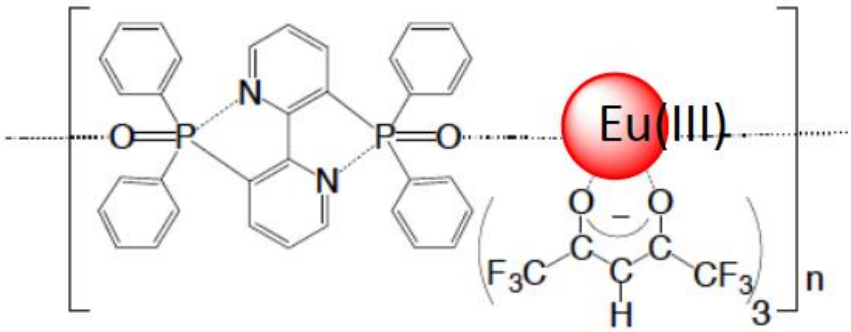

(b)

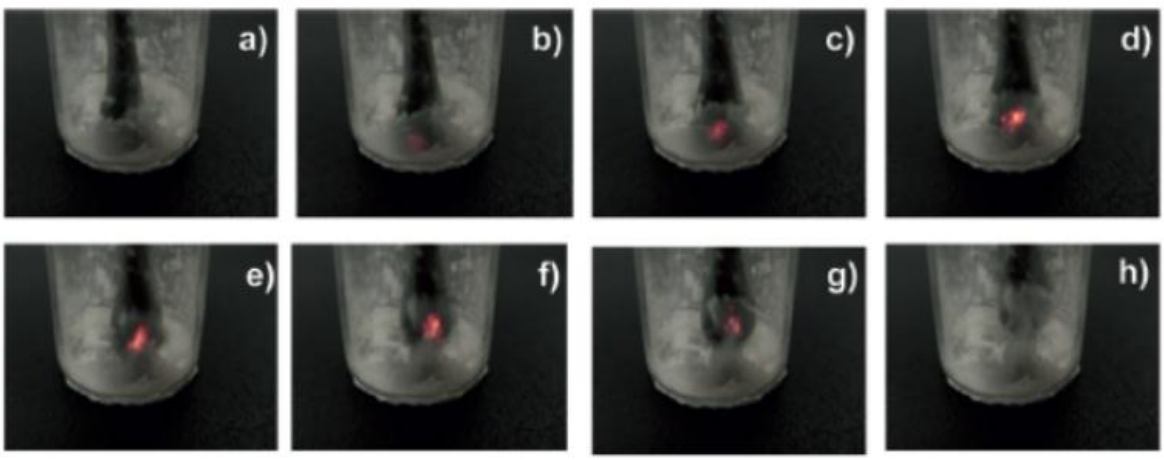

T. Hasegawa and T. Nakanishi, Fig.11

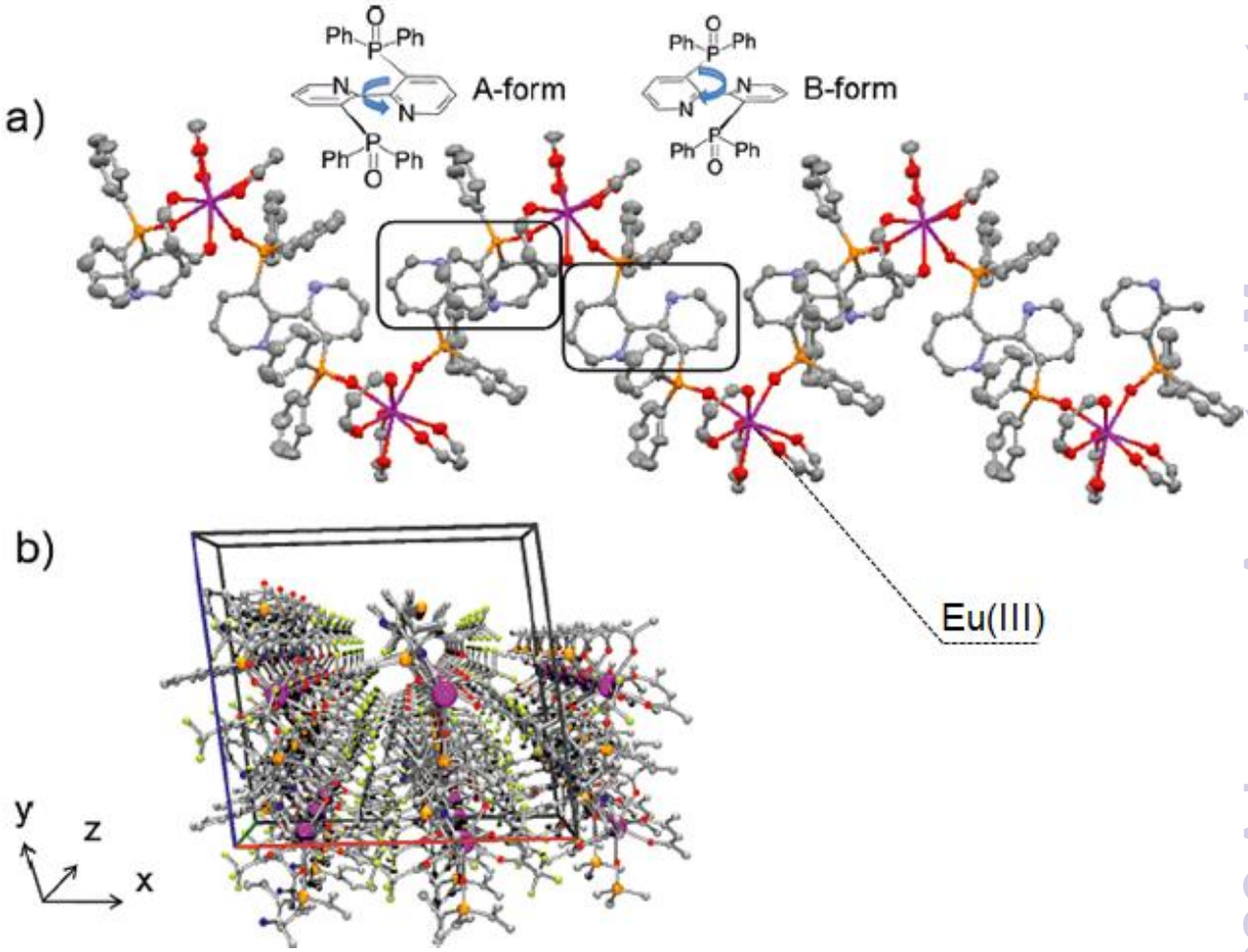

Y. Hasegawa and T. Nakanishi, Fig.12

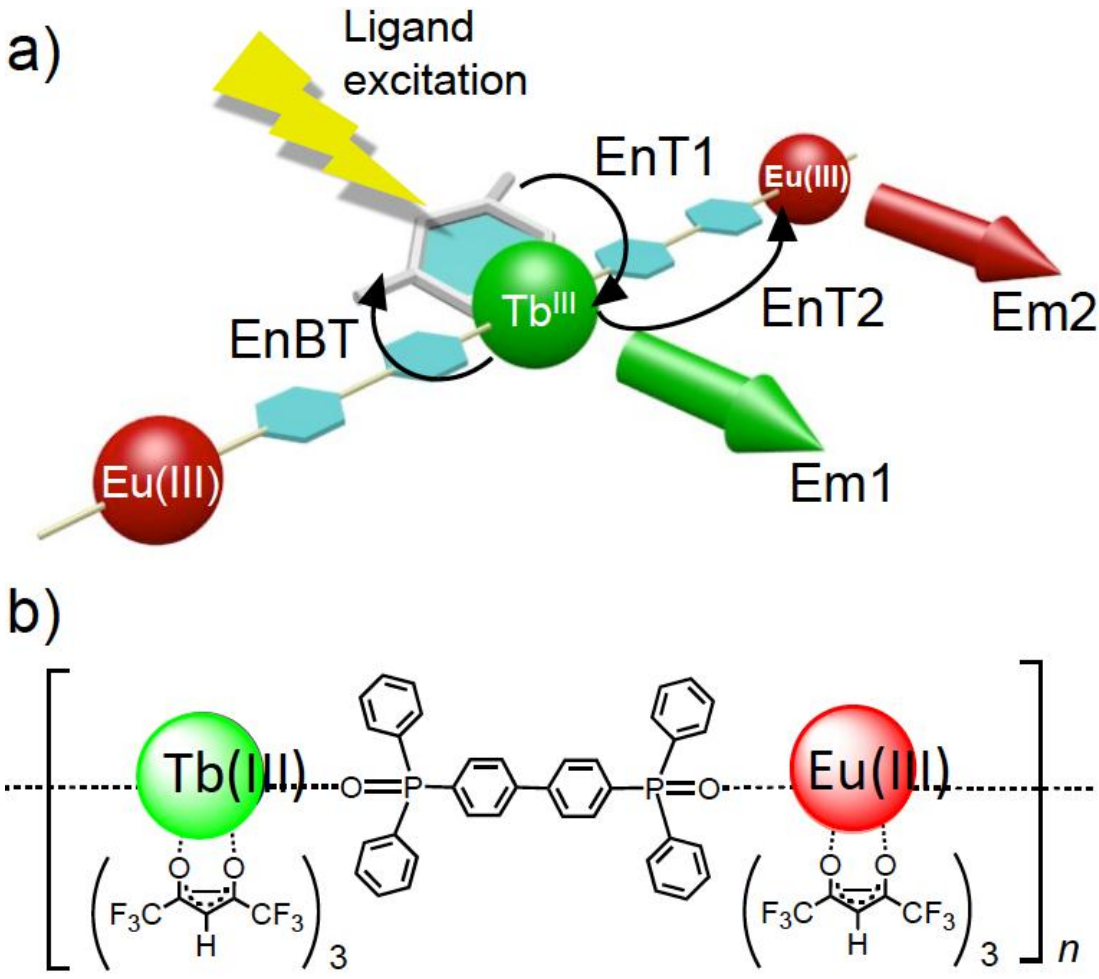

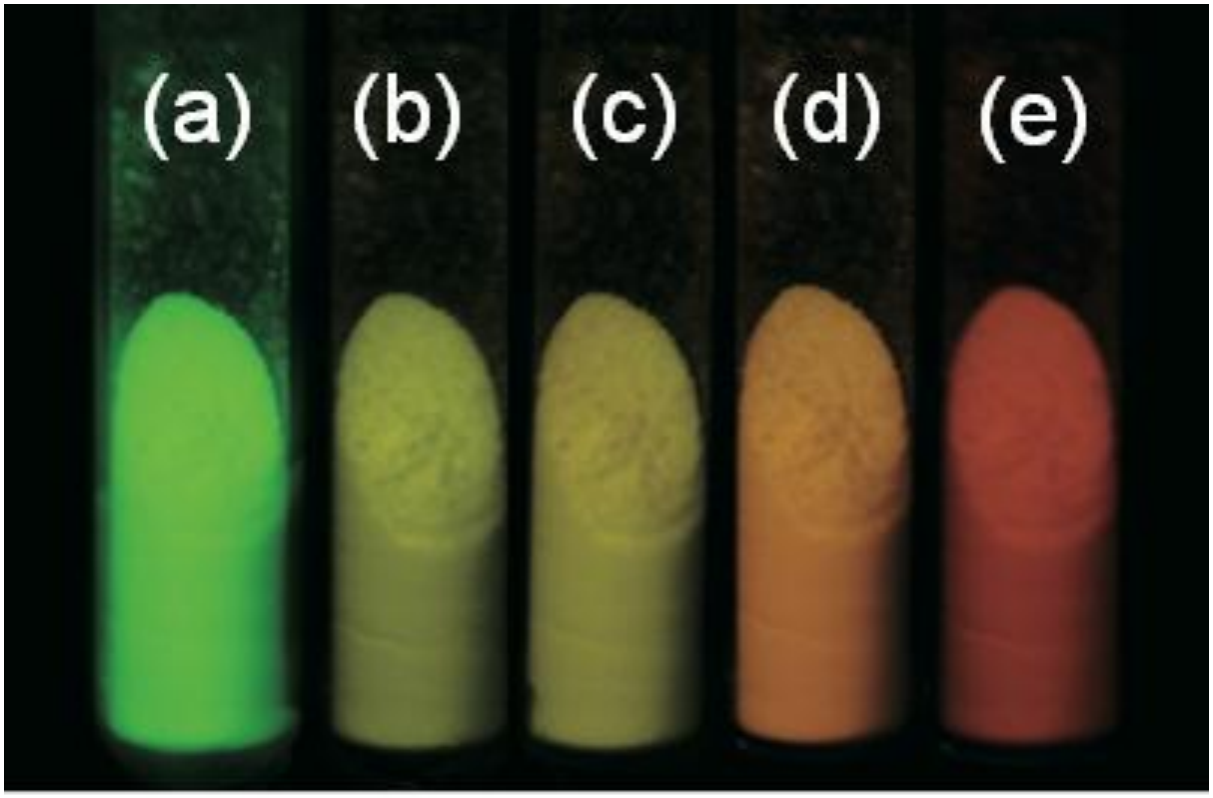

Y. Hasegawa and T. Nakanishi, Fig.14

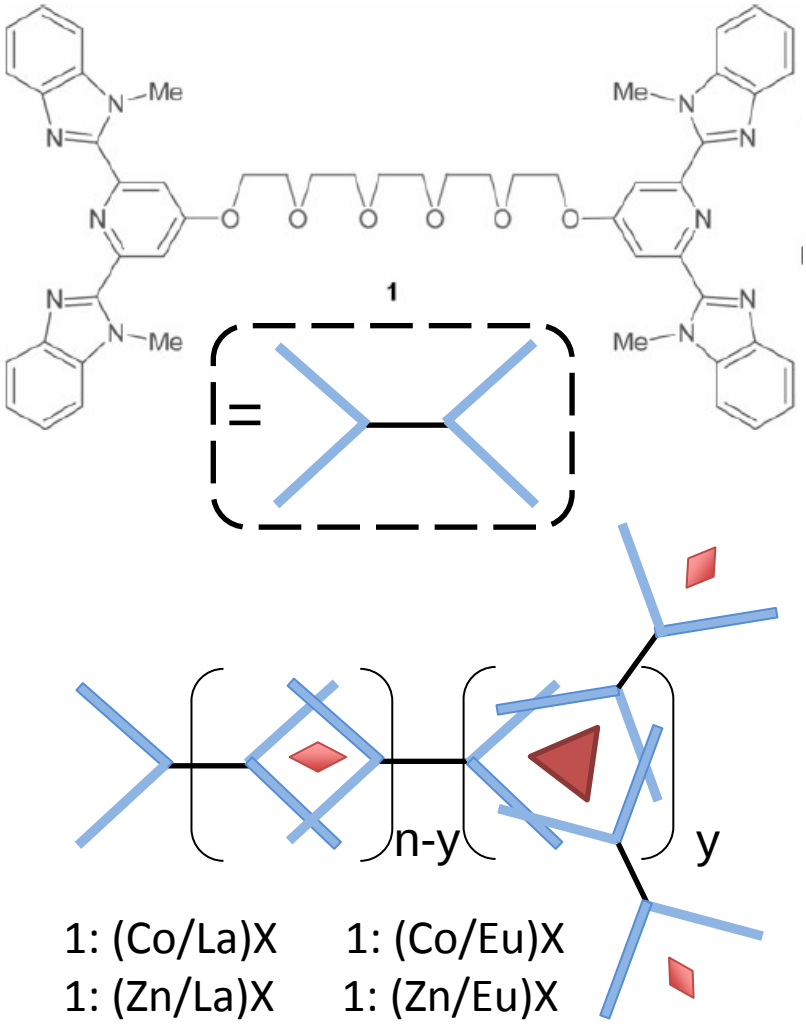

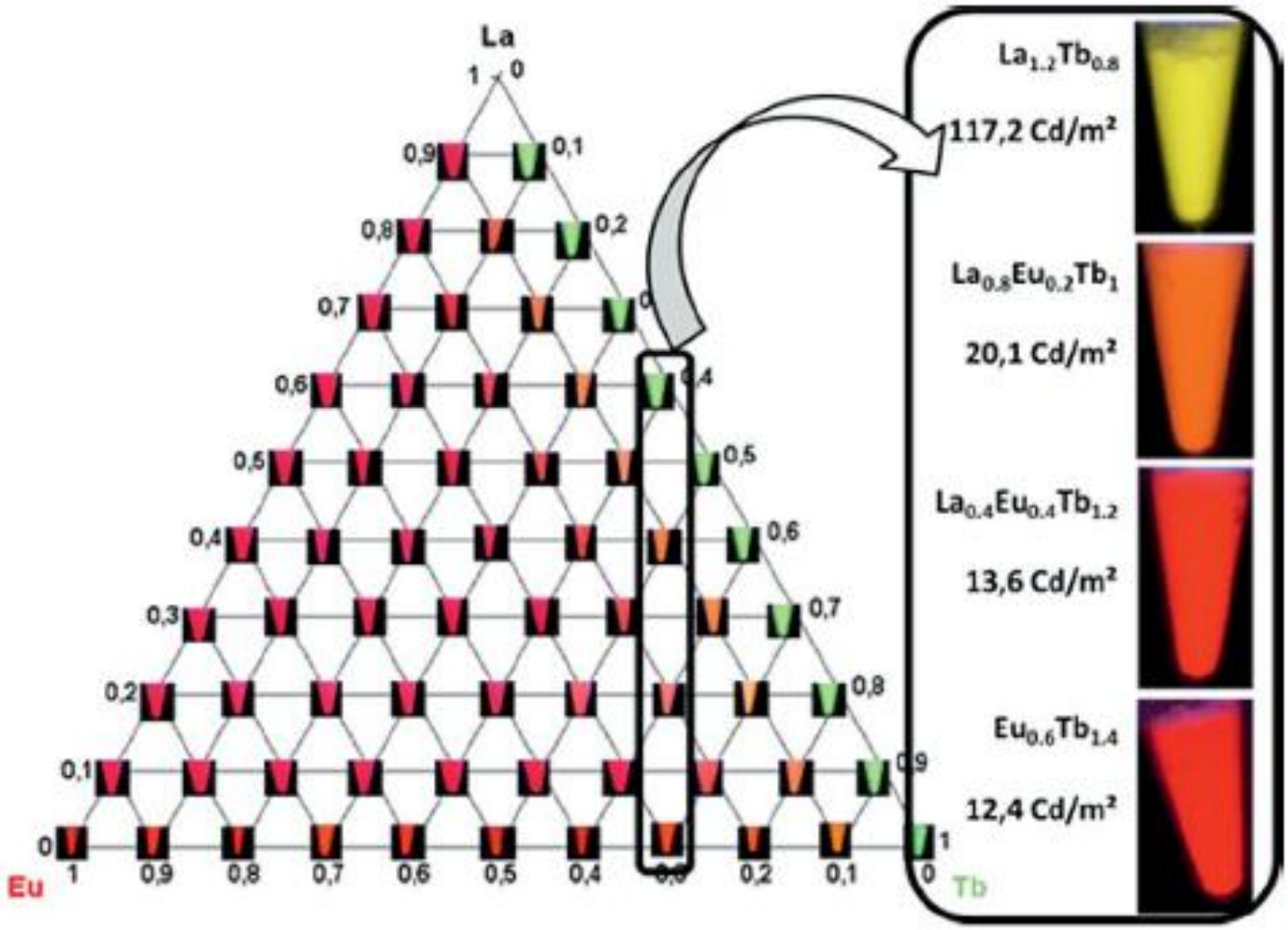

Y. Hasegawa and T. Nakanishi, Fig.16

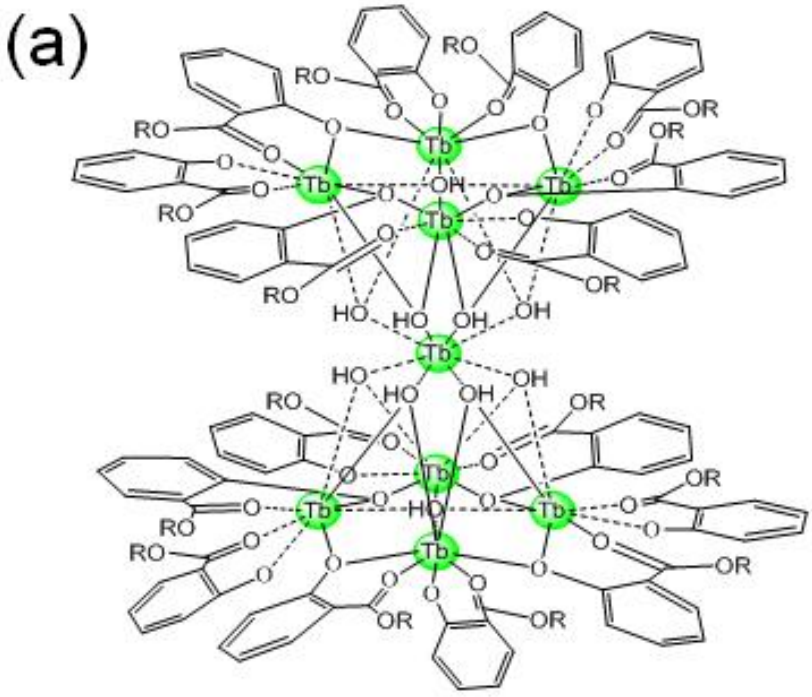

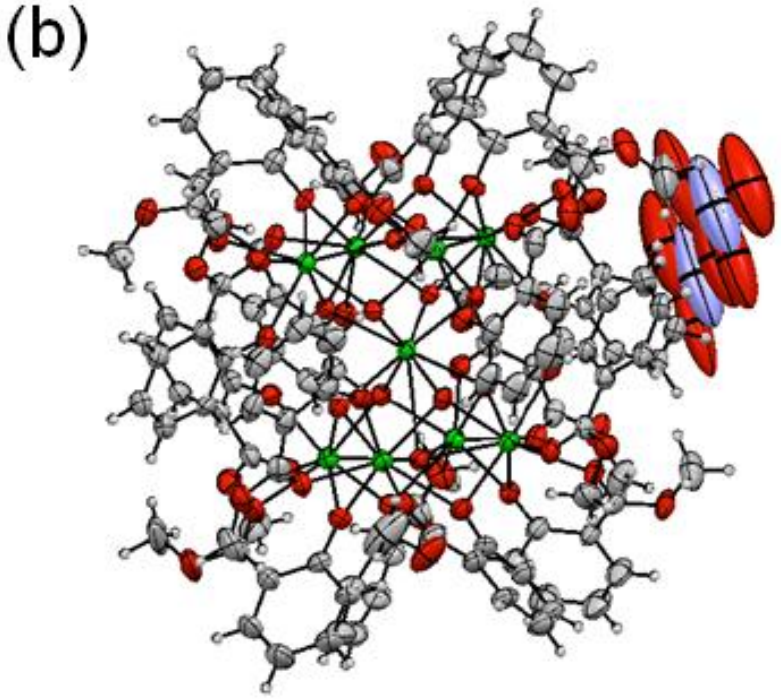

8-SAP

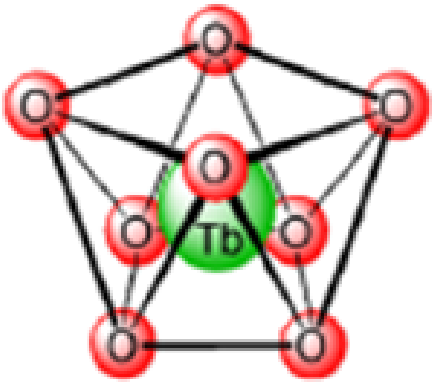

8-TDH

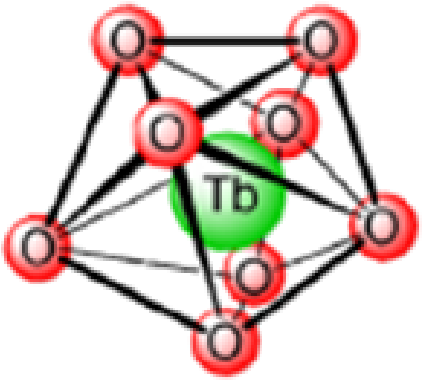

Y. Hasegawa and T. Nakanishi, Fig.18

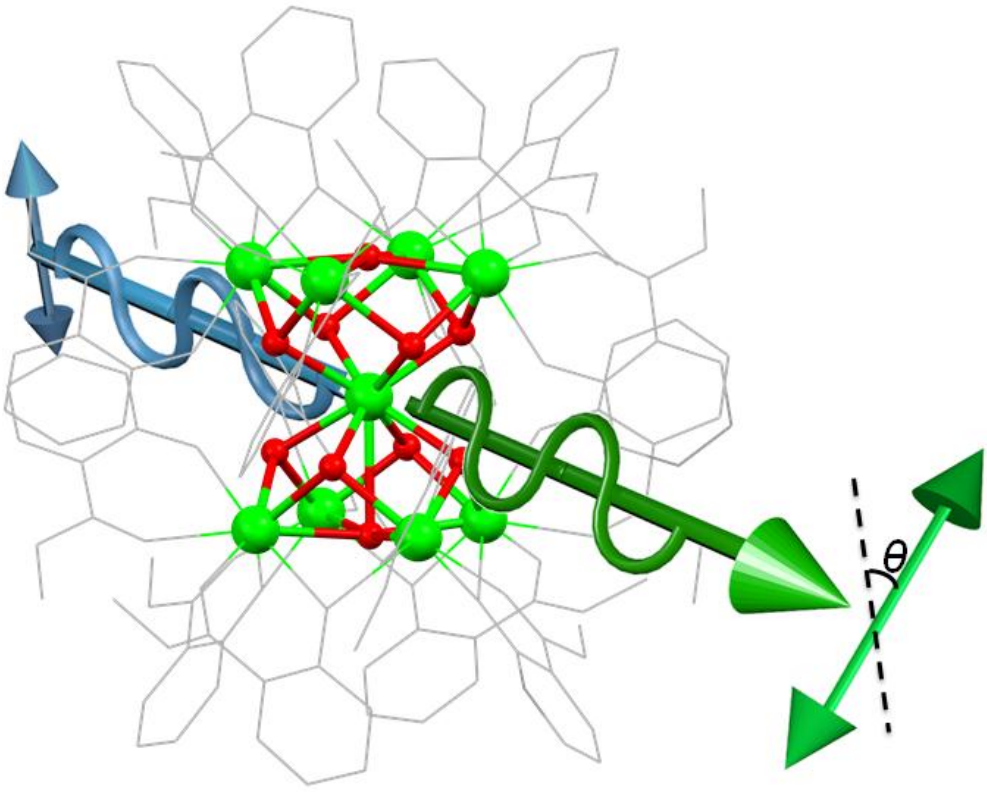

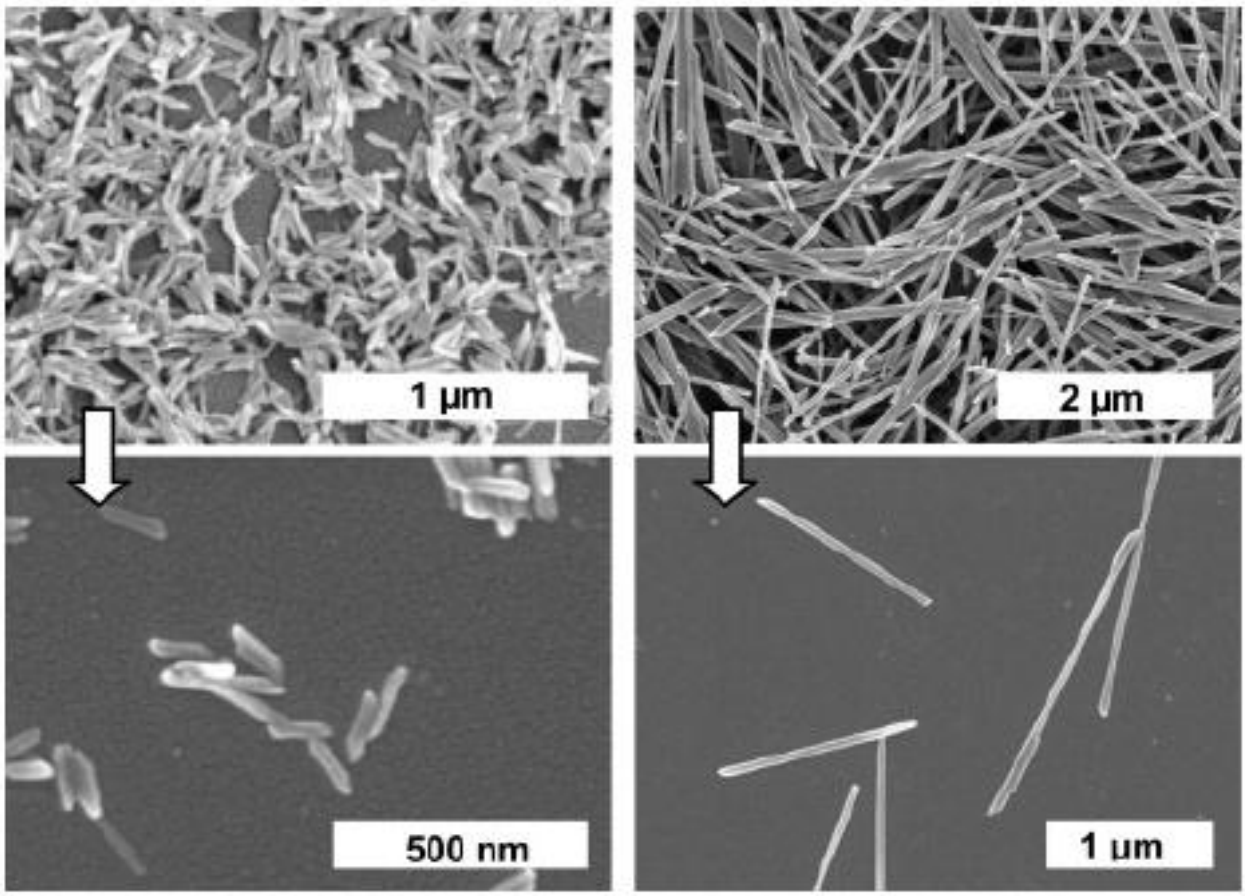

Y. Hasegawa and T. Nakanishi, Fig.20

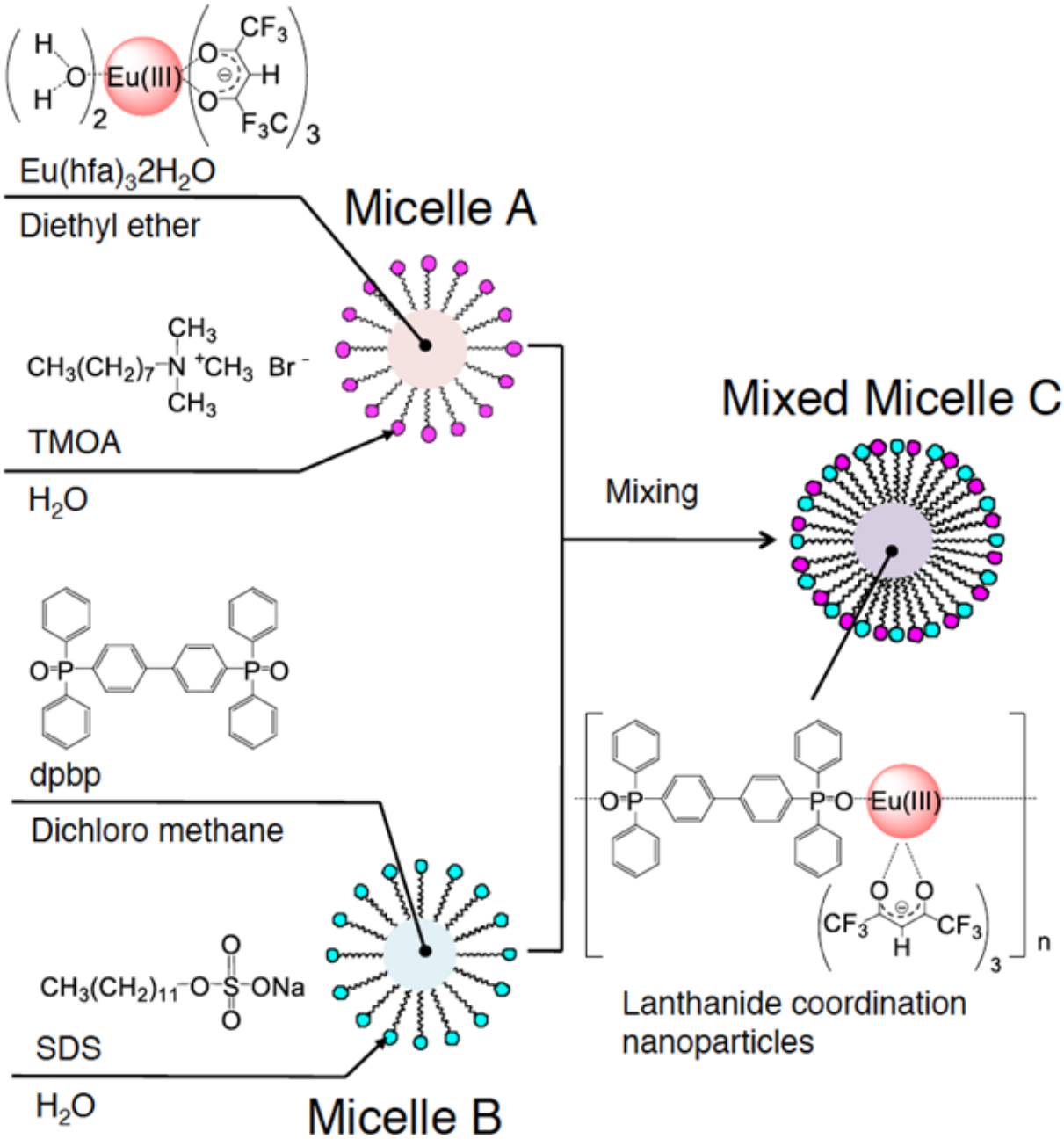

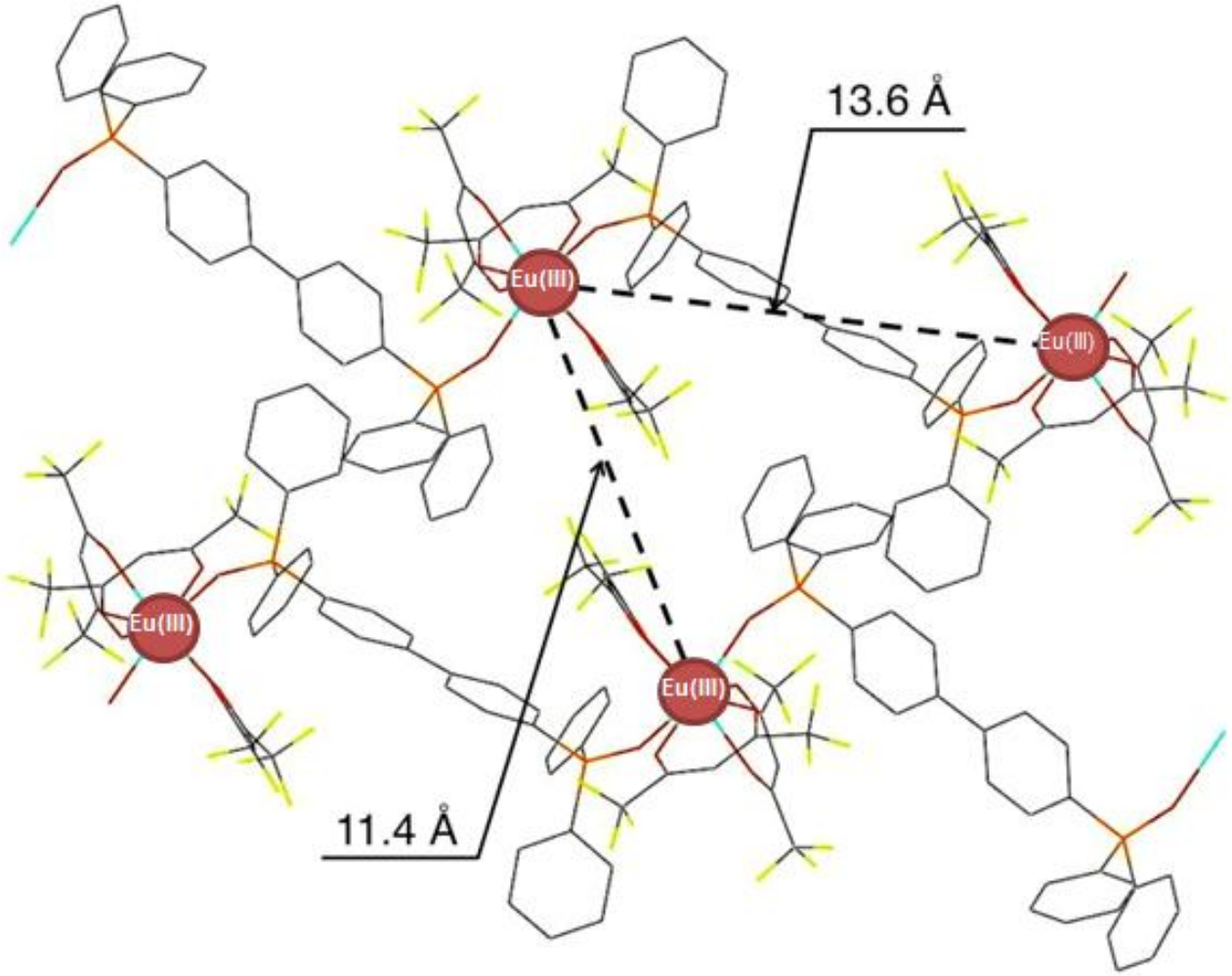

Y. Hasegawa and T. Nakanishi, Fig.22